

# StyleDomain: Analysis of StyleSpace for Domain Adaptation of StyleGAN

Aibek Alanov<sup>1,2,\*</sup>, Vadim Titov<sup>2,\*</sup>, Maksim Nakhodnov<sup>2,\*</sup>, Dmitry Vetrov<sup>1,2</sup>

<sup>1</sup>HSE University <sup>2</sup>AIRI

aalanov@hse.ru, titov@2a2i.org, nakhodnov@2a2i.org, dvetrov@hse.ru

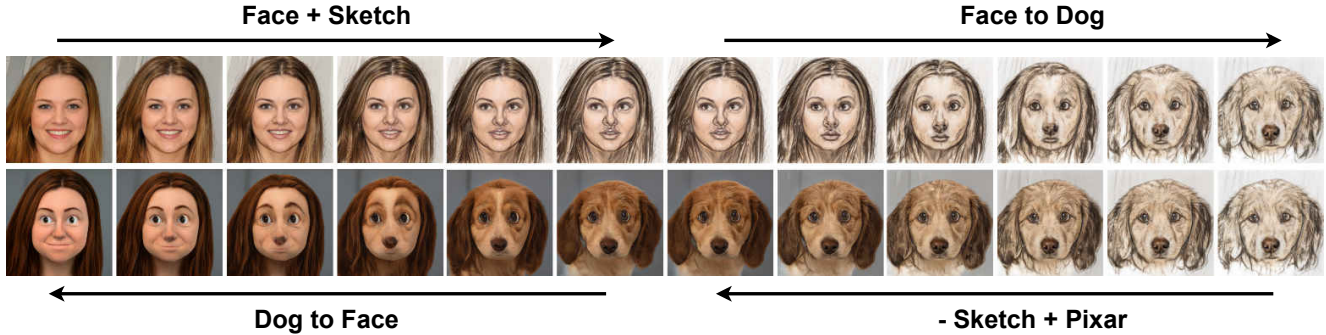


Figure 1. Smooth cross-domain image morphing. Morphing in the space of generator weights could be successfully combined with morphing using StyleDomain directions, i.e. directions in the StyleSpace that can adapt the generator to new domains (see Section 4).

## Abstract

Domain adaptation of GANs is a problem of fine-tuning the state-of-the-art GAN models (e.g. StyleGAN) pretrained on a large dataset to a specific domain with few samples (e.g. painting faces, sketches, etc.). While there are a great number of methods that tackle this problem in different ways there are still many important questions that remain unanswered. In this paper, we provide a systematic and in-depth analysis of the domain adaptation problem of GANs, focusing on the StyleGAN model. First, we perform a detailed exploration of the most important parts of StyleGAN that are responsible for adapting the generator to a new domain depending on the similarity between the source and target domains. In particular, we show that affine layers of StyleGAN can be sufficient for fine-tuning to similar domains. Second, inspired by these findings, we investigate StyleSpace to utilize it for domain adaptation. We show that there exist directions in the StyleSpace that can adapt StyleGAN to new domains. Further, we examine these directions and discover their many surprising properties. Finally, we leverage our analysis and findings to deliver practical improvements and applications in such standard tasks as image-to-image translation and cross-domain morphing.

\*Equal contribution

## 1. Introduction

Recent years GANs [5, 10, 17–19] show impressive results in image synthesis and offer many ways of control over generated data. In particular, the state-of-the-art StyleGAN models [17–19] have many practical applications such as image enhancement [6, 22, 39, 44], image editing [1, 12, 15, 27, 33, 35, 41], image-to-image translation [9, 14, 29, 34] thanks to their high-quality image generation and their latent representation that has rich semantics and disentangled controls for localized meaningful image manipulations. However, it comes at a price as the training of StyleGAN requires a large high-quality dataset that significantly limits its applicability because there are many real-world domains are represented by only few images. The standard approach to deal with this problem is transfer learning, i.e. fine-tuning the model pretrained on the source domain  $A$  to the target domain  $B$ .

There are many domain adaptation methods for StyleGAN [4, 9, 16, 21, 26, 29, 37, 42, 43, 46, 47, 50] that tackle this problem in different ways depending on the similarity between source  $A$  and target  $B$  domains. Most of these works implicitly assume that StyleGAN can be adapted to a new domain only if we fine-tune almost all its weights. However, this common wisdom is poorly investigated and verified. The paper [42] is the first attempt to perform an in-depth analysis of this question. It examines aligned StyleGAN models, i.e. models when one is fine-tuned from the other

to a new domain. They analyze what parts of StyleGAN are changed mostly during domain adaptation. However, they do not touch on the question of what components of StyleGAN are sufficient for adapting the generator.

In this work, we aim to provide a systematic and comprehensive analysis of this question. Our investigation of the properties of the aligned StyleGAN models consists of several parts. First, in Section 3, we identify what parts of the StyleGAN are sufficient for its adaptation depending on the similarity between source  $A$  and target  $B$  domains. We discover that fine-tuning the synthesis convolutional network is not always necessary. In the case of similar  $A$  and  $B$  domains, the affine layers are sufficient for the adaptation. For dissimilar domains, we can adapt successfully just by adding only one convolutional block from the synthesis network. It suggests investigating the latent space of StyleGAN that is formed by the output of affine layers (i.e., StyleSpace [41]) to utilize it for domain adaptation.

In the second part of our analysis, in Section 4, we explore directions in the StyleSpace that can adapt StyleGAN to other domains. We first show that such directions exist (and we call it *StyleDomain directions*) and for similar target domains they demonstrate the comparable domain adaptation quality as fine-tuning all weights of StyleGAN. Next, we extend StyleSpace and propose a new latent space *StyleSpace+* that allows adapting even to dissimilar domains. Further, we inspect these StyleDomain directions and discover their surprising properties. For example, we show that we can sum up these directions to obtain a new mixed domain (see Figure 8), and the same directions can be successfully applied to other aligned StyleGAN models (see Figure 7).

Additionally, in Section 5, we consider practical improvements and applications that can be delivered by our analysis and findings. First, our study allows choosing the optimal parameter space for domain adaptation depending on the type of target domain. Second, we discover and demonstrate different applications of StyleDomain directions such as mixed domains and transferring adaptation between aligned StyleGAN models. Finally, we apply our findings to standard computer vision tasks such as image-to-image translation and cross-domain morphing. In Section 5 we show that image-to-image translation can be solved by significantly less trainable parameters while achieving the same performance. In addition, we consider complex cross-domain image morphing between various domains that can be easily implemented based on our findings.

## 2. Related Work

**Latent Spaces of StyleGAN.** After recent remarkable success of GANs [5, 10, 17–19] in image synthesis, many works appeared that explore their latent representation for controllable image manipulation. In particular, the latent

space of StyleGAN [17–19] has attracted considerable attention. It consists of three levels: (i) the first latent space,  $\mathcal{Z}$ , is raw random noise (typically Gaussian); (ii) the intermediate latent spaces  $\mathcal{W}, \mathcal{W}+$  [1] are formed by the output of the mapping network; (iii) the last level is StyleSpace,  $\mathcal{S}$ , [41] that is spanned by the channel-wise style parameters after affine layers. It has been shown that these latent spaces have rich semantics [18, 19], and especially the StyleSpace that demonstrates the most disentangled and localized semantical directions [41]. In recent years many works have proposed to utilize such appealing properties of the StyleGAN latent spaces for image editing tasks [1, 12, 15, 27, 33, 35, 41]. To apply these methods for real images it is necessary to inverse them into one of the latent space of StyleGAN which is another task that draws significant attention [1, 11, 19, 28, 31, 36, 48, 49]. We should note that all mentioned methods for image manipulation by controlling StyleGAN latent space allow only in-domain editing. In this paper, we show that in StyleSpace there exist such directions that can change the domain of images.

**Domain Adaptation of StyleGAN.** Recent years the problem of fine-tuning StyleGAN has generated a great deal of interest as it allows training the state-of-the-art generative model for a domain with few samples. There have appeared many works that tackle this problem in different ways depending on how much the target domain is similar to the source one. Roughly, these methods can be divided into two groups. The first one deals with the case when the target and source domains are completely different (e.g. faces  $\rightarrow$  cars, churches, etc.). In contrast, the second group considers the setting of similar domains (e.g. faces  $\rightarrow$  stylized faces, painting faces, sketches, etc.). Methods from the first group typically require hundreds or thousands of samples from new domain to adapt faithfully and they leverage data augmentations [16, 37, 46, 47], or freeze some layers of the discriminator to prevent overfitting [23], or train the discriminator with auxiliary losses to match the data more accurately [21, 43]. In the setting of the second group it is sufficient to have only several samples (up to dozens) from the target domain for the successful adaptation and such approaches utilize another techniques. In particular, they introduce additional regularization terms [20, 38], preserve pairwise distances between instances in the source domain via cross-domain consistency loss [26], mix weights of the fine-tuned and the base generators [29], use an auxiliary small network to enhance the training [40]. More advanced methods [4, 9, 50] utilize the pretrained CLIP model [30] as the vision-language supervision for the text-based adaptation [4, 9] or the one-shot image-based adaptation [4, 50]. There are also methods from the second group that try to reduce the size of the parameter space during fine-tuning process [4, 25, 32]. The work [4] utilizes by several orders less

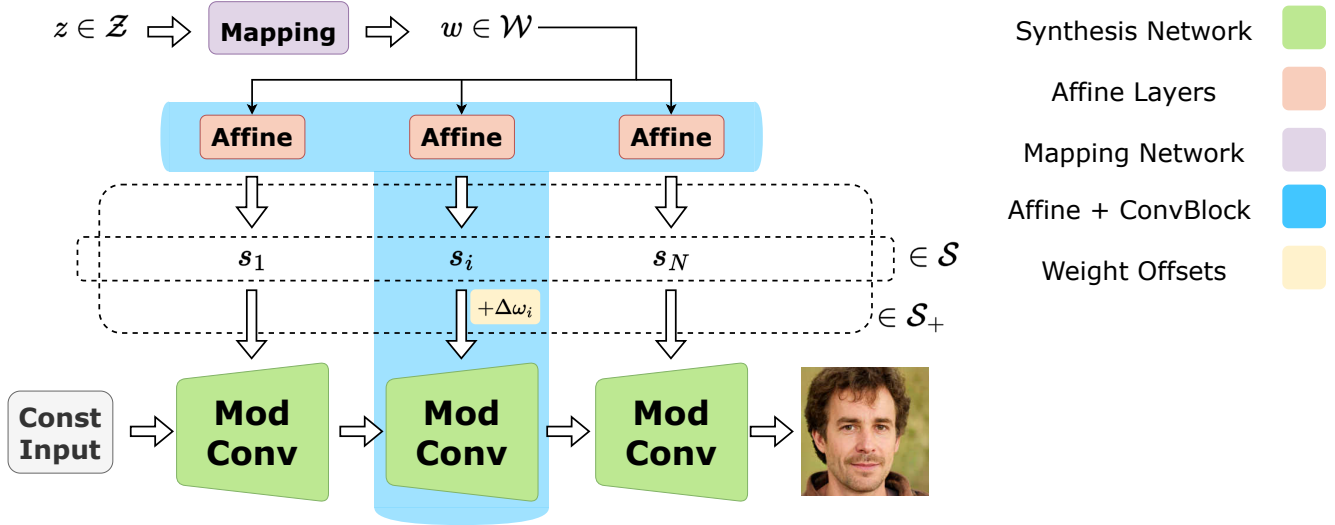


Figure 2. StyleGAN2 architecture. We introduce new latent space  $S+$  for the for domain adaptation that combines StyleSpace and weight offsets for one block from the synthesis network.

parameters and achieves the same expressiveness as models with the full parameter space however it considers only target domains that are similar to the source one.

Although there have been already proposed many methods that deal with the problem of adapting StyleGAN there are still very few works that analyze this process more thoroughly. The paper [42] is the first attempt to perform such in-depth study. They examine the relationship between the base and fine-tuned StyleGAN generators depending on the similarity between source and target domains (they call them aligned models). In particular, they explore which parts of StyleGAN are mostly changed during fine-tuning and the transferability of the latent semantics between aligned models. However, many important questions remain untouched. In our paper, we provide more systematic and comprehensive analysis that completes and improves results from [42].

### 3. Importance of Each Part of the StyleGAN

In this section, our goal is to analyze what parts of StyleGAN are important for domain adaptation. Similarly to previous works we specifically focus on the state-of-the-art GAN architecture, StyleGAN2 [19]. For the source domain, we consider FFHQ [18] as it is the large high-quality dataset that is suitable for training StyleGAN2 from scratch. For the target one, we test a wide range of different domains that we describe further.

**StyleGAN2 structure and its main components.** We provide a diagram description of the StyleGAN2 architecture in Figure 2. It consists of three parts:

- *mapping network*  $f_M$  that transforms the input noise  $z \in \mathcal{Z}$  (typically Gaussian) to the intermediate latent vector  $w \in \mathcal{W}$ ;

- *affine layers*  $f_1^A, \dots, f_N^A$ , each of them takes as input the vector  $w$  and maps it to corresponding style vector  $s_1 = f_1^A(w), \dots, s_N = f_N^A(w)$ . The concatenation of these vectors form the vector from the StyleSpace:  $s = (s_1, \dots, s_N) \in \mathcal{S}$ ;
- *synthesis network* that is a composition of modulated convolutions. The weights of each convolution are modulated by the input style vector  $s_i$  and applied to the input feature maps. The synthesis network also has tRGB convolutional layers that transform feature maps to RGB images and they also are modulated by corresponding style vectors.

Accordingly, the StyleGAN2  $G_\theta$  generates from the input noise  $z$  the output image  $I = G_\theta(f_1^A(f_M(z)), \dots, f_N^A(f_M(z)))$  where  $\theta$  are weights of the synthesis network.

We will analyze these three components of StyleGAN2 and their impact on the domain adaptation process. It is common wisdom that the most important part for adaptation is the synthesis network while the mapping network and affine layers are responsible mostly for the semantic manipulations within the source domain [42]. We aim to verify whether such a conception is correct.

In our experiments, we additionally consider the impact of the combination of affine layers and one convolutional block from the synthesis network on domain adaptation. It is a way to probe the intermediate case between affine layers and the synthesis network.

#### Method to analyze the impact of each component.

The paper [42] has proposed to analyze the impact of each component by resetting its weights in the fine-tuned generator to its pretrained values and assessing the quality of gen-

erated images. In our work, we propose another approach: to directly fine-tune only one of these components to explore which ones are sufficient for domain adaptation.

Let us describe our method in more detail. The optimization process for the problem of domain adaptation is the following

$$\mathcal{L}_D \left( \{G_\theta(s_1^i, \dots, s_N^i)\}_{i=1}^K \right) \rightarrow \min, \quad (1)$$

where  $\mathcal{L}_D$  is domain adaptation loss that depends on the domain  $D$  (we discuss it further) and the samples from the generator  $G_\theta$ ,  $s^1, \dots, s^K \in \mathcal{S}$  are style vectors obtained from sampled noises  $z_1, \dots, z_K \in \mathcal{Z}$ , i.e.  $s^i = (f_1^A(f_M(z_i)), \dots, f_N^A(f_M(z_i)))$ ,  $i = 1, \dots, K$ .

Typically the generator  $G_\theta$  is optimized with respect to all components, i.e.

$$\mathcal{L}_D \left( \{G_\theta(s_1^i, \dots, s_N^i)\}_{i=1}^K \right) \rightarrow \min_{\theta, f^A, f_M}, \quad (2)$$

where  $f^A = \{f_1^A, \dots, f_N^A\}$ .

We propose to investigate settings when we optimize with respect to only one these components. We denote each parameter space as:  $\{\theta\}$  – *SyntConv* parameterization,  $\{f^A\}$  – *Affine* parameterization,  $\{f_M\}$  – *Mapping* parameterization. The case we fine-tune all components of the StyleGAN2 we call *Full* parameterization.

As we discussed above, we propose to consider one additional parameter space as combination of affine layers and one block from synthesis layer with specified spatial resolution. Such block has two convolutional layers with weights  $\theta_1, \theta_2 \in \mathbb{R}^{512 \times 512 \times 3 \times 3}$ . Instead of fine-tuning all these weights we introduce more compact parameterization as offsets  $\Delta\theta_1, \Delta\theta_2$  to these weights that are same across spatial dimensions, i.e.  $\Delta\theta_1, \Delta\theta_2 \in \mathbb{R}^{512 \times 512 \times 1 \times 1}$ . Such parameterization allows us to reduce the number of trainable parameters almost by an order (from 4,7M to 0,5M parameters). In addition to  $\Delta\theta_1, \Delta\theta_2$  we introduce the offsets to the weights  $\theta^{tRGB} \in \mathbb{R}^{3 \times 512 \times 3 \times 3}$  of the tRGB convolutional layer of the same block with similar parameterization  $\Delta\theta^{tRGB} \in \mathbb{R}^{3 \times 512 \times 1 \times 1}$ . Further, we omit such detail about tRGB part in the sake of brevity. So, for this parameterization the optimization procedure has the following form:

$$\mathcal{L}_D \left( \{G_{\theta, \Delta\theta_1, \Delta\theta_2}(s_1^i, \dots, s_N^i)\}_{i=1}^K \right) \rightarrow \min_{\Delta\theta_1, \Delta\theta_2, f^A}, \quad (3)$$

where  $G_{\Delta\theta_1, \Delta\theta_2}$  is the generator with weight offsets  $\Delta\theta_1, \Delta\theta_2$  for the one block from the synthesis network.

We call such parameter space as *Affine+*. We examine all blocks of the synthesis network to choose for this parameterization. We end up with the block with  $64 \times 64$  resolution as it shows the best performance (see results of this analysis in Appendix).

**Types of domains.** In our study, we consider three types of domains depending on its similarity to the source domain of realistic faces from FFHQ:

- *similar* domains: it has the same geometry of faces and it preserves the identity of the person. It alters only the style of the image. Examples of such domains are text-based adaptations with the text description "Photo in the style of anime (pixar, sketch, etc.)" or one-shot image-based adaptation with different stylized face images (see examples in Figure 3).
- *moderately similar* domains: it has face-like form but changes the face geometry and identity in a stronger manner. As examples we consider the following datasets: MetFaces [16], Mega cartoon dataset [29], Ukiyo-e faces [29], AFHQ dogs faces and cats faces [7] (see images in Figure 4).
- *dissimilar* domains: it does not have even face-like structure. We take as examples the following domains: LSUN Car and Church [45], Flowers [24] (see images in Figure 4).

Depending on the type of domain  $D$  we use different domain loss function  $\mathcal{L}_D$ . For similar domains we apply the optimization loss from [9] in the case of text-based adaptation and another loss from [50] for one-shot image-based adaptation. For moderately similar and dissimilar domains we utilize the fine-tuning procedure from [16]. For more details about domain adaptation loss functions see Appendix A.1.

To obtain quantitative comparisons in the case of similar domains we use Quality and Diversity metrics that were proposed in the work [4]. For other two types of domains we compute FID metric [13] using the standard protocol from [16].

**Analysis for similar domains.** For the analysis we choose different text-based and one-shot image-based domains (see Appendix A.2 for the full list and for more details). In experiments we consider four parameterizations (Full, SyntConv, Affine, Mapping) we discussed above.

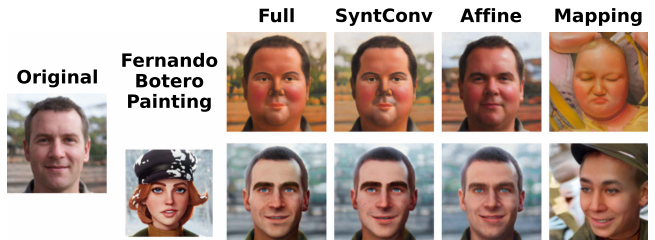


Figure 3. Text-based and image-based adaptation for different parameterizations. Affine parameterization yields performance comparable with Full one. This style image is called "Anastasia".



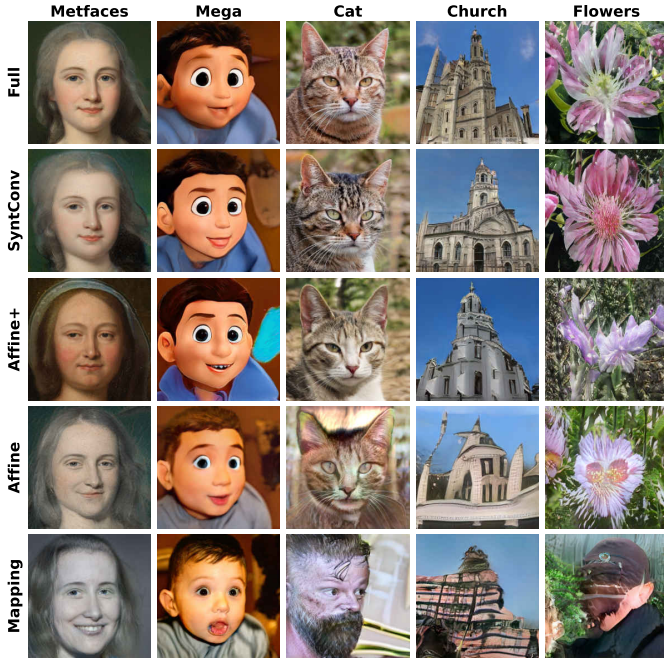


Figure 4. Domain adaptation for moderately similar and dissimilar domains. Affine+ parameterization produce results on par with Full one even for dissimilar domains (Cat, Church).

We provide qualitative results in Figure 3 with quantitative ones in Table 1. More results see in Appendix A.2.

We observe that all three parameterizations Full, SyntConv and Affine show comparable performance in terms of both visual quality and objective metrics. The fact that the synthesis network is sufficient for similar domains was clear from the previous work [42]. However, our finding that affine part is also sufficient is a new and surprising result. It means that we can change the domain of generated images without fine-tuning the synthesis network but just passing the modified style vector that comes from the affine part. Also we observe that the mapping network shows poor visual quality and low diversity in the generated images considering Diversity metric. It indicates that for the successful

adaptation it is important to update the style vector from  $S$  rather than the intermediate latent vector from  $\mathcal{W}$  space.

For similar domains we do not show results for Affine+ parameterization because Affine already achieves the same quality as the Full parameterization. In our experiments, we observe that Affine+ demonstrates the same performance as Affine.

**Analysis for moderately similar domains.** For this setting as we discussed above, we consider five datasets (MetFaces, Mega, Ukiyo-e faces, AFHQ Dogs and Cats) and the results are provided in Figure 4 and in Table 2. See more results in Appendix A.3.

For moderately similar domains we see that results are different compared to similar ones. In particular, we observe that Affine parameterization does not demonstrate the same quality as the full parameterization. It can be seen from degraded visual quality and visible gap in FID metric. However, it is still surprising that the generated images after adaptation have adequate visual appearance considering that we do not fine-tune the synthesis network at all. It is even more surprising that Affine+ parameterization allows removing this performance gap from the Full parameterization both qualitatively and quantitatively. While the number of parameters for the additional block in Affine+ accounts for only 2 % of the synthesis network size. It shows that the style vector allows adapting the generator even to more distant domains if we just add the small part of the synthesis network.

SyntConv expectedly achieves results comparable with Full parameterization, and Mapping conversely shows poor quality on all domains.

**Analysis for dissimilar domains.** For this setting we take three datasets (Cars, Churches and Flowers) and the results are provided in Figure 4 and in Table 2. See more results in Appendix A.3.

In this case we notice that Affine+ parameterization shows slightly worse results than Full one. The quantitative gap is significant only for Cars domain while for Churches and Flowers it is negligible. It confirms that for the successful adaptation of StyleGAN2 even to dissimilar domains it

Table 1. Quality and Diversity metrics [4] for text-based and one-shot image-based domain adaptations with different parameterizations. Affine and StyleSpace parameterizations achieve results comparable with Full parameterization.

Parameter Space	Size	Botero		Sketch		The Joker		Anastasia (image)	
		Quality	Diversity	Quality	Diversity	Quality	Diversity	Quality	Diversity
Full	30.3M	0.312	0.228	0.208	0.296	0.246	0.167	0.640	0.276
SyntConv	23.6M	0.311	0.224	0.191	0.292	0.245	0.164	0.683	0.250
Affine	4.6M	0.298	0.221	0.194	0.296	0.244	0.168	0.642	0.269
Mapping	2.1M	0.226	0.115	0.182	0.143	0.246	0.136	0.523	0.202
StyleSpace	9K	0.309	0.23	0.193	0.306	0.242	0.187	0.616	0.296

Table 2. FID scores for domain adaptation with different parameterizations. We observe a significant gap between Affine and Full parameterizations that, however, can be drastically reduced by introducing weight offsets for the single synthesis block.

Parameter Space	Size	Metfaces	Mega	Ukiyoe	Dog	Cat	Car	Church	Flowers
Full	30.3M	21.9	81.1	22.6	20.3	7.1	25.6	18.1	17.0
SyntConv	23.6M	22.8	82.5	24.7	19.7	7.2	25.1	18.0	17.4
Affine+	5.1M	22.1	78.2	26.8	18.6	7.0	43.5	18.8	18.0
Affine	4.6M	25.9	108.8	63.5	70.1	27.6	116.3	88.3	42.6
Mapping	2.1M	54.9	137.3	159.8	208.2	226.1	245.0	268.6	236.4

is sufficient only to fine-tune the small fraction of its all parameters.

The Affine parameterization shows significant degradation in the quality for this case that leads to the conclusion that for dissimilar domains it is important to fine-tune at least some part of the synthesis network. For SyntConv and Mapping parameterization, we observe expected results.

#### 4. StyleSpace for Domain Adaptation

**Exploring directions in the StyleSpace for adapting StyleGAN.** Our findings from the previous section suggest an idea that we can change the domain of generated images by modifying the style vector from the StyleSpace  $\mathcal{S}$ . To check this hypothesis, we will adapt StyleGAN2 by directly optimizing the direction in  $\mathcal{S}$ , i.e. during fine-tuning of StyleGAN we will optimize only  $\Delta s^D$ :

$$\mathcal{L}_D \left( \{G_\theta(s_1^i + \Delta s_1^D, \dots, s_N^i + \Delta s_N^D)\}_{i=1}^K \right) \rightarrow \min_{\Delta s^D} \quad (4)$$

where  $\Delta s^D = (\Delta s_1^D, \dots, \Delta s_N^D) \in \mathcal{S}$  is the optimized direction in the  $\mathcal{S}$  for adapting the generator  $G_\theta$  to the domain  $D$ . We call such directions  $\Delta s^D$  as *StyleDomain* directions.

We apply such parameterization to each type of domains and obtain the following results.

For similar domains we provide results in Figure 5 and in Table 1 (see more results in Appendix A.4). We observe



Figure 5. StyleSpace parameterization performs domain adaptation comparable with Full parameterization even with 5000 times less trained parameters.

that optimizing the StyleDomain direction  $\Delta s^D$  achieves the same results both visually and quantitatively as the Full parameterization. It is new and important observation that StyleSpace allows not only image editing within domain but also generating samples from out-of domain.

For experiments with other two types of domains we extend the StyleSpace and introduce new space *StyleSpace+*  $\mathcal{S}+$  as the Cartesian product of StyleSpace and the space of weight offsets  $\Delta\theta_1, \Delta\theta_2$  to the one block from the synthesis network with resolution  $64 \times 64$  (see Section 3). Specifically,  $\mathcal{S}+ = \mathcal{S} \times \mathbb{R}^{512 \times 512 \times 1 \times 1} \times \mathbb{R}^{512 \times 512 \times 1 \times 1}$ , i.e. during fine-tuning process we optimize the vector  $\Delta s_+^D = (\Delta s^D, \Delta\theta_1, \Delta\theta_2) \in \mathcal{S}+$ :

$$\mathcal{L}_D \left( \{G_{\theta, \Delta\theta_1, \Delta\theta_2}(s_1^i + \Delta s_1^D, \dots, s_N^i + \Delta s_N^D)\}_{i=1}^K \right) \rightarrow \min_{\Delta\theta_1, \Delta\theta_2, \Delta s^D} \quad (5)$$

So, for moderately similar and dissimilar domains we provide results in Figure 6 and in Table 3 (see more results in Appendix A.4). We observe that the domain adaptation in

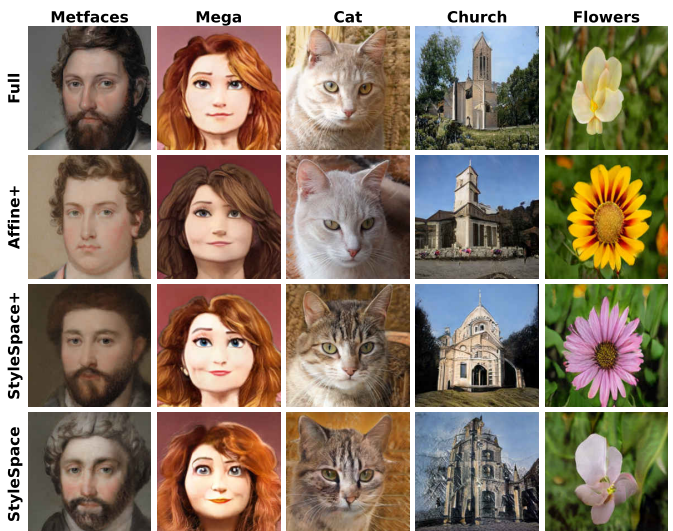


Figure 6. Domain adaptation for moderately similar and dissimilar domains. StyleSpace+ parameterization closes the gap in quality for all presented domains despite having 60 times less trainable parameters.

Table 3. FID scores for domain adaptation in  $\mathcal{S}$  and  $\mathcal{S}+$ . StyleSpace+ parameterization can be competitive for moderately similar domains (Metfaces, Mega).

Parameter Space	Size	Metfaces	Mega	Ukiyoe	Dog	Cat	Car	Church	Flowers
Full	30.3M	21.9	81.1	22.6	20.3	7.1	25.6	18.1	17.0
StyleSpace+	0.5M	25.3	83.2	32.5	29.4	9.1	46.2	28.7	22.3
StyleSpace	9.0K	30.3	102.7	52.0	75.8	22.0	138.7	66.4	39.0

$\mathcal{S}$  works much worse for this case compared to Full parameterization. However, we should notice that it still shows reasonable quality considering that it has only 9 thousand training parameters which is less by several orders than 30 million parameters in Full parameterization.

Optimizing in  $\mathcal{S}+$  allows reducing this performance gap and it is minimal for moderately similar domains. For dissimilar domains we see a noticeable degradation in quality. It means that for this case we need more parameters to fine-tune.

**Properties of the StyleSpace domain directions.** We show that in  $\mathcal{S}$  and  $\mathcal{S}+$  there exist such StyleDomain directions that can adapt the generator to similar and moderately similar domains correspondingly. In this part, we explore its properties in detail.

First, we investigate whether we can transfer StyleDomain directions between aligned StyleGAN2 models. In particular, let us consider the base generator  $G_\theta$  pretrained on realistic faces and the generator  $G_\theta^{Dog}$  fine-tuned to domain of dogs in the Full parameterization. We aim to verify whether we could apply StyleDomain directions to  $G_\theta^{Dog}$  if they were optimized for  $G_\theta$ . Specifically, we conduct the following experiment. At first, we take StyleDomain directions that were optimized for  $G_\theta$  to adapt it to different text-based and one-shot image-based domains (e.g. Pixar, Anastasia, etc.). Next, we apply these directions to generators that were fine-tuned from  $G_\theta$  to other domains (e.g. MetFaces, Mega, Dogs, etc.). We provide results of this ex-

periment in Figure 7 (see more results in Appendix A.5). We see that for moderately similar domains the StyleDomain directions can be successfully transferred. For dissimilar domains the visual quality is less satisfactory but reasonable.

Second, we discover that StyleDomain directions can be combined with each other. In particular, we can consider several directions that correspond to different similar domains and take their linear combination. The resulting direction will adapt the generator to the semantically mixed domain. We provide different examples of such combinations in Figure 8 (see more results in Appendix A.5).

Finally, we check that StyleDomain directions can be successfully combined with latent controls for image editing. For more detail exploration of this property see in Appendix A.5.

## 5. Practical Benefits of Our Findings

**Immediate practical benefits.** Our analysis and explored properties of aligned StyleGAN2 models deliver the following practical benefits:

- we significantly reduce the size of parameterization for domain adaption. For the case of similar domains, we explore StyleDomain directions that have 9 thousand trainable parameters compared to 30 million weights of the Full parameterization. For the case of moderately similar domains, we propose StyleSpace+ that

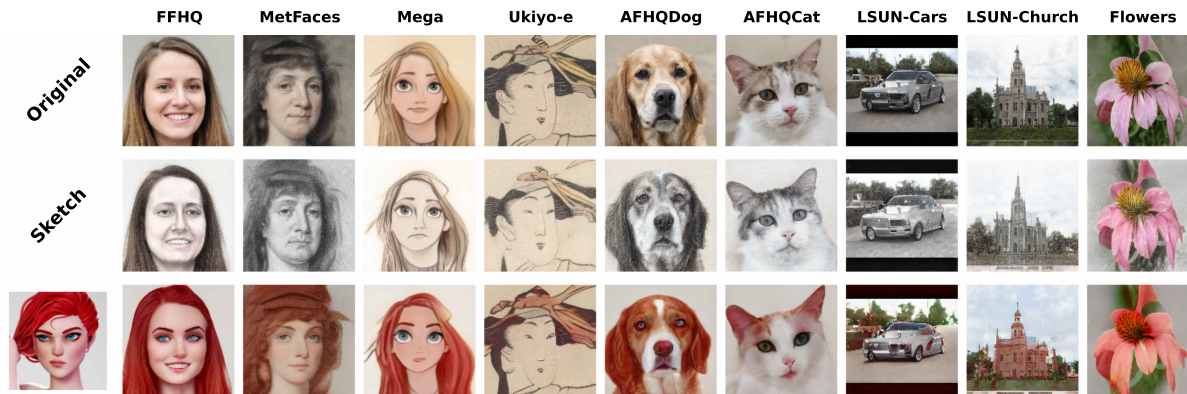


Figure 7. StyleSpace directions transfer from text-based and image-based domain adaptation to other fine-tuned models. We can successfully transfer style while preserving image content.





Figure 8. Example of mixing StyleDomain directions. We can combine different directions in order to perform adaptation into a semantically mixed domain.

has only half a million parameters.

- we discover the transferability of StyleDomain directions to other aligned StyleGAN2 models. It gives the opportunity to apply directions found for one generator to all its child models. We show its wide applicability in Figure 7 and in Appendix A.5.
- we explore the ability of StyleDomain directions to be combined with each other to produce mixed domains. It opens the opportunity to create many interesting combinations of different domains. We demonstrate examples in Figure 8 and in Appendix A.5.

In addition to these applications, we consider two standard tasks from the computer vision and provide more efficient solutions.

**Cross-domain image translation.** We consider two setups of standard image-to-image problem. In the first one, we translate images from the source domain to the target domain unconditionally. In the second setup, we perform a reference-based translation, where the resulting image combines the pose and the shape of the source image with the style from a reference image.

To solve this task, we exploit the model alignment of two generators independently fine-tuned to the source and target domains. Following [42] we employ their two-step approach (see details in Appendix A.6).

We compare performance for three parameterizations: Full, Affine+ and StyleSpace+ on both setups, using different pairs of source and target domains from the AFHQ dataset. We report the total number of fine-tuned parameters in both generators as well as the FID and KID scores between the generated images and the train split of the corresponding AFHQ dataset (see details and results for different datasets in Appendix A.6).

The table in Figure 9 shows the gap in quality between StyleSpace+ and Full parameterizations which, however,



Space	Size	I2I		Ref-based I2I	
		FID	KID $\times 10^3$	FID	KID $\times 10^3$
Full	60.6M	18.6	2.78	7.64	2.22
Affine+	10.2M	18.4	2.37	8.44	2.53
StyleSpace+	1.1M	21.5	5.00	10.6	3.43

Figure 9. Comparison of I2I for different parameterizations. Unconditional I2I (the first row) demonstrates the ability to capture the pose and the style from the source image. For reference-based I2I (the second row) all variants produce realistic images that combine pose and structure from the source image with texture and color from the reference.

does not greatly affect the quality of the generated images. For unconditional I2I, all three parameterizations produce realistic results in the target domain and successfully capture high-level semantics from the source image, like style and pose. For reference-based I2I even the StyleSpace+ generator successfully preserves the pose from the source image and the style from the reference image despite having 60 times fewer trainable parameters than the Full parametrization.

**Cross-domain image morphing.** Cross-domain morphing is smooth transition between two images from different domains. This task is known as challenging [3, 8] and it is successfully tackled in the work [42] using aligned StyleGAN2 models. The idea is to interpolate between aligned generator weights to obtain a smooth transition between domains. We propose more complex image morphing by utilizing the transferability of StyleDomain directions. For example, we can apply a direction that stands for Sketch or Pixar style to Dogs domain to obtain smooth transition between sketchy and pixar-like dog (see Figure 1). See many examples of such complex cross-domain morphing in Appendix A.7.

## 6. Conclusion

In this paper, we provide an extensive analysis of the process of StyleGAN domain adaptation. We reveal the sufficient components of the generator for successful adaptation depending on the similarity between the source and target domains. We discover the ability of StyleSpace to change



the domain of generated images by StyleDomain directions. Further, we explore and leverage properties of these directions. We believe that our investigation can attract more attention to the exploration of new interesting properties of StyleSpace.

## References

- [1] Rameen Abdal, Yipeng Qin, and Peter Wonka. Image2stylegan: How to embed images into the stylegan latent space? In *Proceedings of the IEEE/CVF International Conference on Computer Vision*, pages 4432–4441, 2019. 1, 2
- [2] Rameen Abdal, Peihao Zhu, Niloy J Mitra, and Peter Wonka. Styleflow: Attribute-conditioned exploration of stylegan-generated images using conditional continuous normalizing flows. *ACM Transactions on Graphics (ToG)*, 40(3):1–21, 2021. 34
- [3] Kfir Aberman, Jing Liao, Mingyi Shi, Dani Lischinski, Baoquan Chen, and Daniel Cohen-Or. Neural best-buddies: Sparse cross-domain correspondence. *ACM Transactions on Graphics (TOG)*, 37(4):1–14, 2018. 8
- [4] Aibek Alanov, Vadim Titov, and Dmitry Vetrov. Hyperdomainnet: Universal domain adaptation for generative adversarial networks. *arXiv preprint arXiv:2210.08884*, 2022. 1, 2, 4, 5, 12, 13, 23
- [5] Andrew Brock, Jeff Donahue, and Karen Simonyan. Large scale gan training for high fidelity natural image synthesis. *arXiv preprint arXiv:1809.11096*, 2018. 1, 2
- [6] Kelvin CK Chan, Xintao Wang, Xiangyu Xu, Jinwei Gu, and Chen Change Loy. Glean: Generative latent bank for large-factor image super-resolution. In *Proceedings of the IEEE/CVF conference on computer vision and pattern recognition*, pages 14245–14254, 2021. 1
- [7] Yunjey Choi, Youngjung Uh, Jaejun Yoo, and Jung-Woo Ha. Stargan v2: Diverse image synthesis for multiple domains. In *Proceedings of the IEEE/CVF conference on computer vision and pattern recognition*, pages 8188–8197, 2020. 4
- [8] Noa Fish, Richard Zhang, Lilach Perry, Daniel Cohen-Or, Eli Shechtman, and Connelly Barnes. Image morphing with perceptual constraints and stn alignment. In *Computer Graphics Forum*, volume 39, pages 303–313. Wiley Online Library, 2020. 8
- [9] Rinon Gal, Or Patashnik, Haggai Maron, Amit H Bermano, Gal Chechik, and Daniel Cohen-Or. Stylegan-nada: Clip-guided domain adaptation of image generators. *ACM Transactions on Graphics (TOG)*, 41(4):1–13, 2022. 1, 2, 4, 11
- [10] Ian Goodfellow, Jean Pouget-Abadie, Mehdi Mirza, Bing Xu, David Warde-Farley, Sherjil Ozair, Aaron Courville, and Yoshua Bengio. Generative adversarial nets. *Advances in neural information processing systems*, 27, 2014. 1, 2
- [11] Shanyan Guan, Ying Tai, Bingbing Ni, Feida Zhu, Feiyue Huang, and Xiaokang Yang. Collaborative learning for faster stylegan embedding. *arXiv preprint arXiv:2007.01758*, 2020. 2
- [12] Erik Härkönen, Aaron Hertzmann, Jaakko Lehtinen, and Sylvain Paris. Ganspace: Discovering interpretable gan controls. *Advances in Neural Information Processing Systems*, 33:9841–9850, 2020. 1, 2
- [13] Martin Heusel, Hubert Ramsauer, Thomas Unterthiner, Bernhard Nessler, and Sepp Hochreiter. Gans trained by a two time-scale update rule converge to a local nash equilibrium. *Advances in neural information processing systems*, 30, 2017. 4
- [14] Jialu Huang, Jing Liao, and Sam Kwong. Unsupervised image-to-image translation via pre-trained stylegan2 network. *IEEE Transactions on Multimedia*, 24:1435–1448, 2021. 1
- [15] Ali Jahanian, Lucy Chai, and Phillip Isola. On the “steerability” of generative adversarial networks. *arXiv preprint arXiv:1907.07171*, 2019. 1, 2
- [16] Tero Karras, Miika Aittala, Janne Hellsten, Samuli Laine, Jaakko Lehtinen, and Timo Aila. Training generative adversarial networks with limited data. *Advances in Neural Information Processing Systems*, 33:12104–12114, 2020. 1, 2, 4, 11
- [17] Tero Karras, Miika Aittala, Samuli Laine, Erik Härkönen, Janne Hellsten, Jaakko Lehtinen, and Timo Aila. Alias-free generative adversarial networks. *Advances in Neural Information Processing Systems*, 34, 2021. 1, 2
- [18] Tero Karras, Samuli Laine, and Timo Aila. A style-based generator architecture for generative adversarial networks. In *Proceedings of the IEEE/CVF conference on computer vision and pattern recognition*, pages 4401–4410, 2019. 1, 2, 3
- [19] Tero Karras, Samuli Laine, Miika Aittala, Janne Hellsten, Jaakko Lehtinen, and Timo Aila. Analyzing and improving the image quality of stylegan. In *Proceedings of the IEEE/CVF conference on computer vision and pattern recognition*, pages 8110–8119, 2020. 1, 2, 3, 11
- [20] Yijun Li, Richard Zhang, Jingwan Lu, and Eli Shechtman. Few-shot image generation with elastic weight consolidation. *arXiv preprint arXiv:2012.02780*, 2020. 2
- [21] Bingchen Liu, Yizhe Zhu, Kunpeng Song, and Ahmed Elgammal. Towards faster and stabilized gan training for high-fidelity few-shot image synthesis. In *International Conference on Learning Representations*, 2020. 1, 2
- [22] Xuan Luo, Xuaner Zhang, Paul Yoo, Ricardo Martin-Brualla, Jason Lawrence, and Steven M Seitz. Time-travel rephotography. *ACM Transactions on Graphics (TOG)*, 40(6):1–12, 2021. 1
- [23] Sangwoo Mo, Minsu Cho, and Jinwoo Shin. Freeze the discriminator: a simple baseline for fine-tuning gans. *arXiv preprint arXiv:2002.10964*, 2020. 2
- [24] M-E Nilsback and Andrew Zisserman. A visual vocabulary for flower classification. In *2006 IEEE Computer Society Conference on Computer Vision and Pattern Recognition (CVPR’06)*, volume 2, pages 1447–1454. IEEE, 2006. 4
- [25] Atsuhiko Noguchi and Tatsuya Harada. Image generation from small datasets via batch statistics adaptation. In *Proceedings of the IEEE/CVF International Conference on Computer Vision*, pages 2750–2758, 2019. 2
- [26] Utkarsh Ojha, Yijun Li, Jingwan Lu, Alexei A Efros, Yong Jae Lee, Eli Shechtman, and Richard Zhang. Few-shot image generation via cross-domain correspondence. In *Proceedings of the IEEE/CVF Conference on Computer Vision and Pattern Recognition*, pages 10743–10752, 2021. 1, 2

- [27] Or Patashnik, Zongze Wu, Eli Shechtman, Daniel Cohen-Or, and Dani Lischinski. Styleclip: Text-driven manipulation of stylegan imagery. In *Proceedings of the IEEE/CVF International Conference on Computer Vision*, pages 2085–2094, 2021. 1, 2
- [28] Stanislav Pidhorskyi, Donald A Adjeroh, and Gianfranco Doretto. Adversarial latent autoencoders. In *Proceedings of the IEEE/CVF Conference on Computer Vision and Pattern Recognition*, pages 14104–14113, 2020. 2
- [29] Justin NM Pinkney and Doron Adler. Resolution dependent gan interpolation for controllable image synthesis between domains. *arXiv preprint arXiv:2010.05334*, 2020. 1, 2, 4
- [30] Alec Radford, Jong Wook Kim, Chris Hallacy, Aditya Ramesh, Gabriel Goh, Sandhini Agarwal, Girish Sastry, Amanda Askell, Pamela Mishkin, Jack Clark, et al. Learning transferable visual models from natural language supervision. In *International Conference on Machine Learning*, pages 8748–8763. PMLR, 2021. 2, 11, 12
- [31] Elad Richardson, Yuval Alaluf, Or Patashnik, Yotam Nitzan, Yaniv Azar, Stav Shapiro, and Daniel Cohen-Or. Encoding in style: a stylegan encoder for image-to-image translation. In *Proceedings of the IEEE/CVF conference on computer vision and pattern recognition*, pages 2287–2296, 2021. 2
- [32] Esther Robb, Wen-Sheng Chu, Abhishek Kumar, and Jiabin Huang. Few-shot adaptation of generative adversarial networks. *arXiv preprint arXiv:2010.11943*, 2020. 2
- [33] Yujun Shen, Jinjin Gu, Xiaouo Tang, and Bolei Zhou. Interpreting the latent space of gans for semantic face editing. In *Proceedings of the IEEE/CVF conference on computer vision and pattern recognition*, pages 9243–9252, 2020. 1, 2, 32
- [34] Guoxian Song, Linjie Luo, Jing Liu, Wan-Chun Ma, Chunpong Lai, Chuanxia Zheng, and Tat-Jen Cham. Agilegan: stylizing portraits by inversion-consistent transfer learning. *ACM Transactions on Graphics (TOG)*, 40(4):1–13, 2021. 1
- [35] Ayush Tewari, Mohamed Elgharib, Gaurav Bharaj, Florian Bernard, Hans-Peter Seidel, Patrick Pérez, Michael Zollhofer, and Christian Theobalt. Stylerig: Rigging stylegan for 3d control over portrait images. In *Proceedings of the IEEE/CVF Conference on Computer Vision and Pattern Recognition*, pages 6142–6151, 2020. 1, 2
- [36] Omer Tov, Yuval Alaluf, Yotam Nitzan, Or Patashnik, and Daniel Cohen-Or. Designing an encoder for stylegan image manipulation. *ACM Transactions on Graphics (TOG)*, 40(4):1–14, 2021. 2
- [37] Ngoc-Trung Tran, Viet-Hung Tran, Ngoc-Bao Nguyen, Trung-Kien Nguyen, and Ngai-Man Cheung. On data augmentation for gan training. *IEEE Transactions on Image Processing*, 30:1882–1897, 2021. 1, 2, 11
- [38] Hung-Yu Tseng, Lu Jiang, Ce Liu, Ming-Hsuan Yang, and Weilong Yang. Regularizing generative adversarial networks under limited data. In *Proceedings of the IEEE/CVF Conference on Computer Vision and Pattern Recognition*, pages 7921–7931, 2021. 2
- [39] Xintao Wang, Yu Li, Honglun Zhang, and Ying Shan. Towards real-world blind face restoration with generative facial prior. In *Proceedings of the IEEE/CVF Conference on Computer Vision and Pattern Recognition*, pages 9168–9178, 2021. 1
- [40] Yaxing Wang, Abel Gonzalez-Garcia, David Berga, Luis Herranz, Fahad Shahbaz Khan, and Joost van de Weijer. Minegan: effective knowledge transfer from gans to target domains with few images. In *Proceedings of the IEEE/CVF Conference on Computer Vision and Pattern Recognition*, pages 9332–9341, 2020. 2
- [41] Zongze Wu, Dani Lischinski, and Eli Shechtman. Stylespace analysis: Disentangled controls for stylegan image generation. In *Proceedings of the IEEE/CVF Conference on Computer Vision and Pattern Recognition*, pages 12863–12872, 2021. 1, 2, 32, 34
- [42] Zongze Wu, Yotam Nitzan, Eli Shechtman, and Dani Lischinski. Stylealign: Analysis and applications of aligned stylegan models. *arXiv preprint arXiv:2110.11323*, 2021. 1, 3, 5, 8, 35
- [43] Ceyuan Yang, Yujun Shen, Yinghao Xu, and Bolei Zhou. Data-efficient instance generation from instance discrimination. *Advances in Neural Information Processing Systems*, 34:9378–9390, 2021. 1, 2
- [44] Tao Yang, Peiran Ren, Xuansong Xie, and Lei Zhang. Gan prior embedded network for blind face restoration in the wild. In *Proceedings of the IEEE/CVF Conference on Computer Vision and Pattern Recognition*, pages 672–681, 2021. 1
- [45] Fisher Yu, Ari Seff, Yinda Zhang, Shuran Song, Thomas Funkhouser, and Jianxiong Xiao. Lsun: Construction of a large-scale image dataset using deep learning with humans in the loop. *arXiv preprint arXiv:1506.03365*, 2015. 4
- [46] Shengyu Zhao, Zhijian Liu, Ji Lin, Jun-Yan Zhu, and Song Han. Differentiable augmentation for data-efficient gan training. *Advances in Neural Information Processing Systems*, 33:7559–7570, 2020. 1, 2, 11
- [47] Zhengli Zhao, Zizhao Zhang, Ting Chen, Sameer Singh, and Han Zhang. Image augmentations for gan training. *arXiv preprint arXiv:2006.02595*, 2020. 1, 2, 11
- [48] Jiapeng Zhu, Yujun Shen, Deli Zhao, and Bolei Zhou. In-domain gan inversion for real image editing. In *European conference on computer vision*, pages 592–608. Springer, 2020. 2
- [49] Jun-Yan Zhu, Philipp Krähenbühl, Eli Shechtman, and Alexei A Efros. Generative visual manipulation on the natural image manifold. In *European conference on computer vision*, pages 597–613. Springer, 2016. 2
- [50] Peihao Zhu, Rameen Abdal, John Femiani, and Peter Wonka. Mind the gap: Domain gap control for single shot domain adaptation for generative adversarial networks. *arXiv preprint arXiv:2110.08398*, 2021. 1, 2, 4, 11

## A. Appendix

### A.1. Domain Adaptation Losses

As we discuss in Section 3, the optimization process for the domain adaptation is

$$\mathcal{L}_D \left( \{G_\theta(s_1^i, \dots, s_N^i)\}_{i=1}^K \right) \rightarrow \min, \quad (6)$$

where  $\mathcal{L}_D$  is the domain adaptation loss that depends on the domain  $D$ . We describe each possible loss function in more detail.

In the case of similar domains, we analyse text-based and one-shot image-based adaptation methods. For the text-based setting, we apply the optimization loss from [9] that equals

$$\mathcal{L}_D \left( \{G_\theta(s_1^i, \dots, s_N^i)\}_{i=1}^K \right) = \sum_{i=1}^K \mathcal{L}_{direction}(G_\theta(s_1^i, \dots, s_N^i)), \quad (7)$$

$$\text{where } \mathcal{L}_{direction}(G_\theta(s_1^i, \dots, s_N^i)) = 1 - \frac{\Delta I_i^T \Delta T}{|\Delta I_i| \cdot |\Delta T|}, \quad (8)$$

$$\Delta I_i = E_I(G_\theta(s_1^i, \dots, s_N^i)) - E_I(G_{\theta_0}(s_1^i, \dots, s_N^i)) \quad (\theta_0 - \text{pretrained weights}), \quad (9)$$

$$\Delta T = E_T(t) - E_T(t_0) \quad (t - \text{text description of the target domain, } t_0 - \text{text description of the source domain}), \quad (10)$$

$$E_I, E_T - \text{pretrained text and image CLIP [30] encoders, respectively} \quad (11)$$

For the one-shot image-based setting, we utilize the loss function from [50] that equals

$$\begin{aligned} \mathcal{L}_D \left( \{G_\theta(s_1^i, \dots, s_N^i)\}_{i=1}^K \right) = & \sum_{i=1}^K (\mathcal{L}_{clip\_across}(G_\theta(s_1^i, \dots, s_N^i)) + \lambda_{cw} \mathcal{L}_{clip\_within}(G_\theta(s_1^i, \dots, s_N^i)) + \\ & + \lambda_{rc} \mathcal{L}_{ref\_clip}(G_\theta(s_1^i, \dots, s_N^i)) + \lambda_{rr} \mathcal{L}_{ref\_rec}(G_\theta(s_1^i, \dots, s_N^i))) \end{aligned} \quad (12)$$

For more details about each loss term  $\mathcal{L}_{clip\_across}$ ,  $\mathcal{L}_{clip\_within}$ ,  $\mathcal{L}_{ref\_clip}$ ,  $\mathcal{L}_{ref\_rec}$  please refer to the original paper [50].

In the case of moderately similar and dissimilar domains, we use the method of fine-tuning GANs using differentiable augmentations [16, 37, 46, 47]. The optimization loss equals

$$\mathcal{L}_D \left( \{G_\theta(s_1^i, \dots, s_N^i)\}_{i=1}^K \right) = \sum_{i=1}^K -D_\varphi(T(G_\theta(s_1^i, \dots, s_N^i))), \quad (13)$$

$$\text{where } T - \text{differentiable augmentation, } D_\varphi - \text{discriminator that is trained using the following loss} \quad (14)$$

$$\left[ \sum_{i=1}^B \max(0, 1 - D_\varphi(T(x_i))) + \sum_{i=1}^B \max(0, 1 + D_\varphi(T(G_\theta(s_1^i, \dots, s_N^i)))) \right] \rightarrow \min_\varphi, \quad (15)$$

$$\text{where } B - \text{batch size, } x_1, \dots, x_B - \text{real samples, } G_\theta(s_1^1, \dots, s_N^1), \dots, G_\theta(s_1^B, \dots, s_N^B) - \text{generated samples.} \quad (16)$$

### A.2. Analysis for Similar Domains

#### A.2.1 Implementation Details

We implement our experiments using PyTorch<sup>1</sup> deep learning framework. For StyleGAN2 [19] architecture in the case of similar domains, we use the popular PyTorch implementation<sup>2</sup>. We attach all source code that reproduces our experiments for the setting with similar domains as a part of the supplementary material named "adaptation\_to\_similar\_domains". We also provide configuration files to run each experiment.

<sup>1</sup><https://pytorch.org>

<sup>2</sup><https://github.com/rosinality/stylegan2-pytorch>

### A.2.2 Hyperparameters

For the text-based domain adaptation we use the optimization loss from Equation (8). As pretrained CLIP Vision-Transformer [30] we utilize "ViT-B/32", "ViT-B/16" models. We use batch size of 4 and different number of iterations depending on the domain (from 250 to 300 iterations). As optimizer we apply the ADAM Optimizer with parameters we provide in Table 4.

For the one-shot image-based domain adaptation we apply the optimization loss from Equation (12). We set loss coefficients as  $\lambda_{cw} = 0.5, \lambda_{rc} = 30, \lambda_{rr} = 10$ . We use batch of 4 and 300 number of iterations. We utilize the ADAM Optimizer with parameters we provide in Table 4.

Table 4. ADAM optimizer hyperparameters for each setting.

Parameter Space	lr	betas	weight_decay
SyntConv	0.002	(0.0, 0.999)	0
Full	0.002	(0.0, 0.999)	0
Affine	0.01	(0.0, 0.999)	0
Mapping	0.3	(0.0, 0.999)	0
StyleSpace	0.05	(0.9, 0.999)	0

### A.2.3 Quantitative Results

For quantitative comparisons, we utilize Quality and Diversity metrics from [4]. The Quality is measured as mean cosine similarity between CLIP embedding of the text description of the target domain and embeddings of generated images from the target domain. In the case of one-shot image-based domain adaptation, the embedding of the target domain is calculated as the CLIP embedding of the reference style image. Diversity metric is estimated as mean pairwise cosine distance between CLIP embeddings of generated images from the target domain. As the CLIP image encoder we use only ViT-L/14 that is not applied during training (in the training we use ViT-B/16, ViT-B/32 image encoders).

For every metric we set the number of synthesized images to **1000**. We evaluate each metric five times with different generated images to estimate error bars. However, we obtain that the error bar is less than  $10^{-5}$  for all settings. So, we omit them in Tables.

We provide calculated metrics in Table 5 for a wide range of domains (text-based and image-based). Please see Figure 10 for the correspondence between the name of style image and its appearance. From the results in Table 5 we see that all four parameterizations Full, SyntConv, Affine and Mapping achieve the comparable Quality but the Mapping has significantly lower Diversity. It indicates that the Mapping parameterization collapsed to one image that maximizes the CLIP score (it can be also seen from qualitative results, see Appendix A.2.4). At the same time, we observe that Affine parameterization demonstrates comparable performance to Full and SyntConv in terms of both Quality and Diversity. It confirms our results from the main part in Section 3 that Affine is sufficient for similar domains.

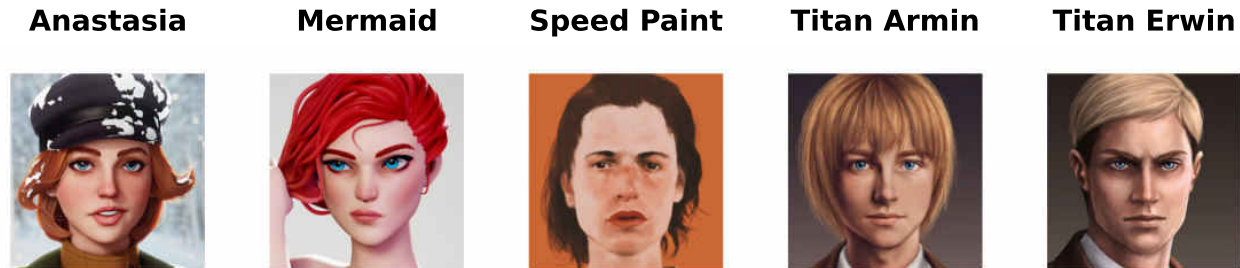


Figure 10. Correspondence between names and style images for one-shot image-based domain adaptation.



Table 5. Quality and Diversity metrics [4] for text-based and one-shot image-based domain adaptation. Affine parameterization achieves comparable results as Full and SyntConv parameterizations.

	Quality				Diversity			
	Full	SyntConv	Affine	Mapping	Full	SyntConv	Affine	Mapping
<b>Text Domains</b>								
Anime Painting	0.25	0.25	0.26	0.22	0.25	0.25	0.23	0.13
Pixar Render	0.27	0.26	0.27	0.26	0.21	0.21	0.20	0.09
Sketch	0.21	0.19	0.19	0.18	0.30	0.31	0.29	0.14
Ukiyo-e Painting	0.22	0.22	0.22	0.23	0.22	0.22	0.23	0.07
Fernando Botero Painting	0.31	0.29	0.29	0.23	0.23	0.24	0.24	0.11
Pop Art	0.25	0.24	0.24	0.26	0.27	0.27	0.33	0.07
Werewolf	0.26	0.25	0.22	0.27	0.13	0.14	0.17	0.07
Zombie	0.24	0.23	0.24	0.24	0.12	0.12	0.13	0.07
The Joker	0.25	0.24	0.24	0.25	0.17	0.17	0.17	0.13
Disney Princess	0.23	0.22	0.23	0.20	0.24	0.28	0.28	0.11
Cubism	0.23	0.21	0.19	0.19	0.22	0.22	0.25	0.07
Tolkien Elf	0.27	0.26	0.28	0.28	0.22	0.23	0.22	0.10
Impressionism	0.27	0.25	0.25	0.24	0.25	0.24	0.25	0.09
Claude Monet	0.21	0.19	0.19	0.22	0.24	0.25	0.27	0.07
Modigliani	0.27	0.25	0.23	0.26	0.20	0.21	0.24	0.12
The Thanos	0.23	0.22	0.23	0.28	0.29	0.31	0.31	0.12
Edvard Munch Painting	0.25	0.23	0.24	0.22	0.20	0.22	0.24	0.09
Dali Painting	0.26	0.24	0.25	0.25	0.22	0.23	0.22	0.14
<b>Image Domains</b>								
Anastasia	0.64	0.67	0.64	0.52	0.28	0.26	0.27	0.20
Mermaid	0.64	0.66	0.63	0.57	0.26	0.25	0.27	0.17
Titan Erwin	0.65	0.64	0.64	0.41	0.28	0.28	0.28	0.14
Titan Armin	0.58	0.57	0.58	0.53	0.29	0.29	0.30	0.10
Speed Paint	0.65	0.65	0.63	0.58	0.31	0.32	0.33	0.12

#### A.2.4 Qualitative Results

We provide more samples for qualitative comparison of different parameterizations. Figures 11 and 12 are extensions of Figure 3 from the Section 3 that show more text-based and image-based domains. Also, we illustrate the diversity of generated samples for each parameterization in Figures 13 to 16. We observe that Full, SyntConv and Affine parameterizations demonstrate comparable visual quality and diversity. While the Mapping parameterization obtains poor adaptation quality and collapsed to one image almost for each domain (see Figure 16). We see that these figures agree with the quantitative results and it confirms the conclusions from Section 3.



Figure 11. Text-based and one-shot image-based domain adaptation for different parameterizations. Affine achieves visual quality on par with Full and SyntConv parameterizations.

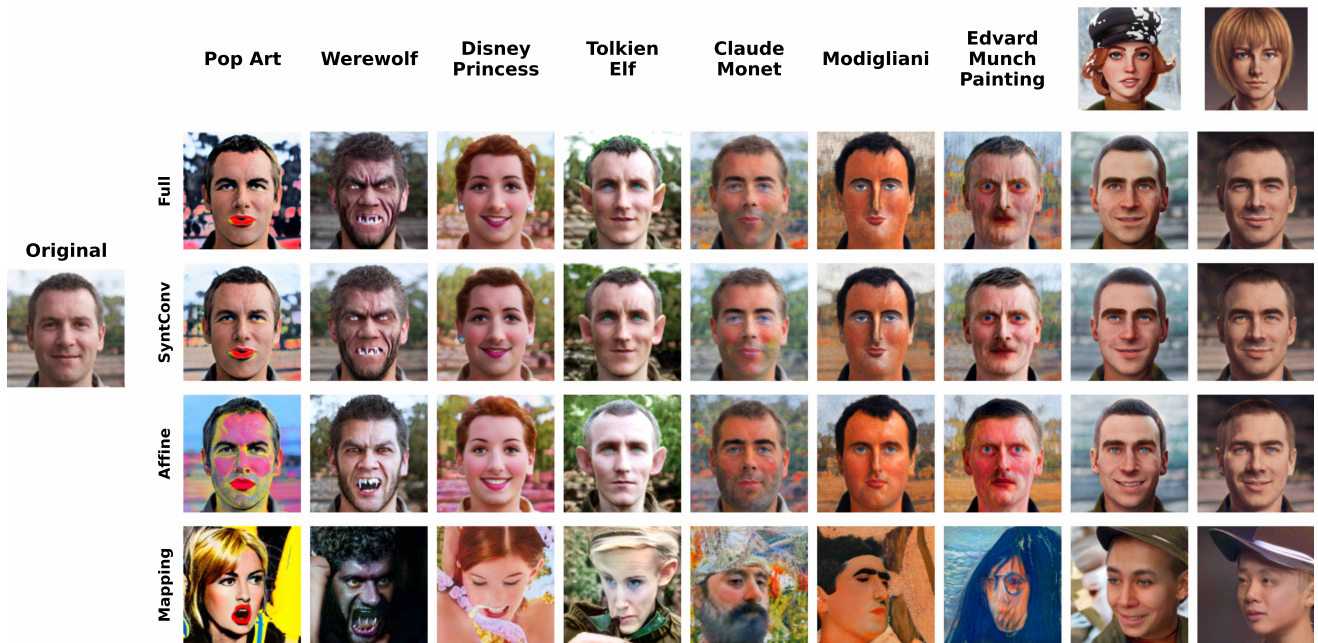


Figure 12. Text-based and one-shot image-based domain adaptation for different parameterizations. Affine achieves visual quality on par with Full and SyntConv parameterizations.





Figure 13. Text-based and one-shot image-based domain adaptation for Affine parameterization. Uncurated random samples for each domain.



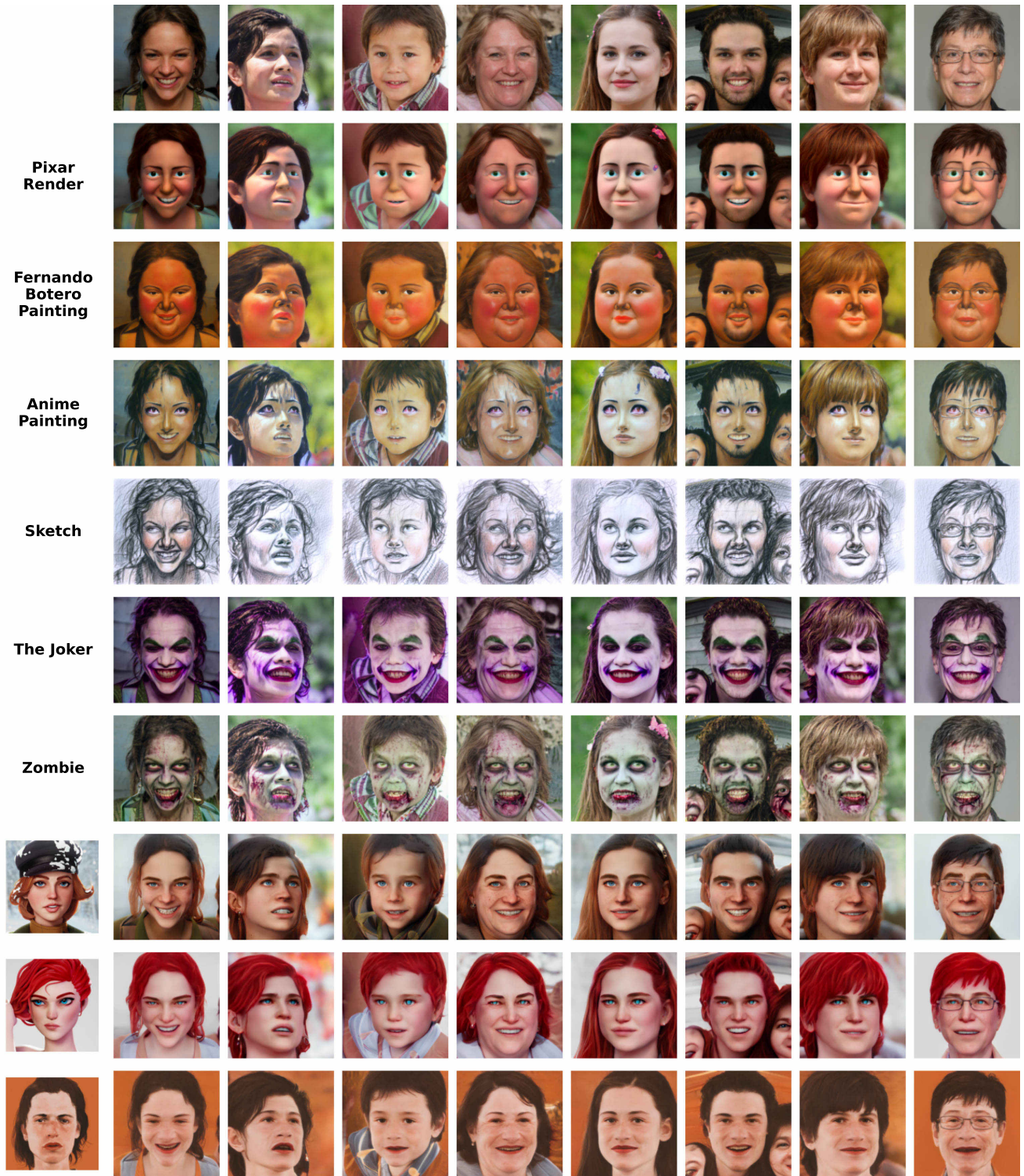


Figure 14. Text-based and one-shot image-based domain adaptation for Full parameterization. Uncurated random samples for each domain.



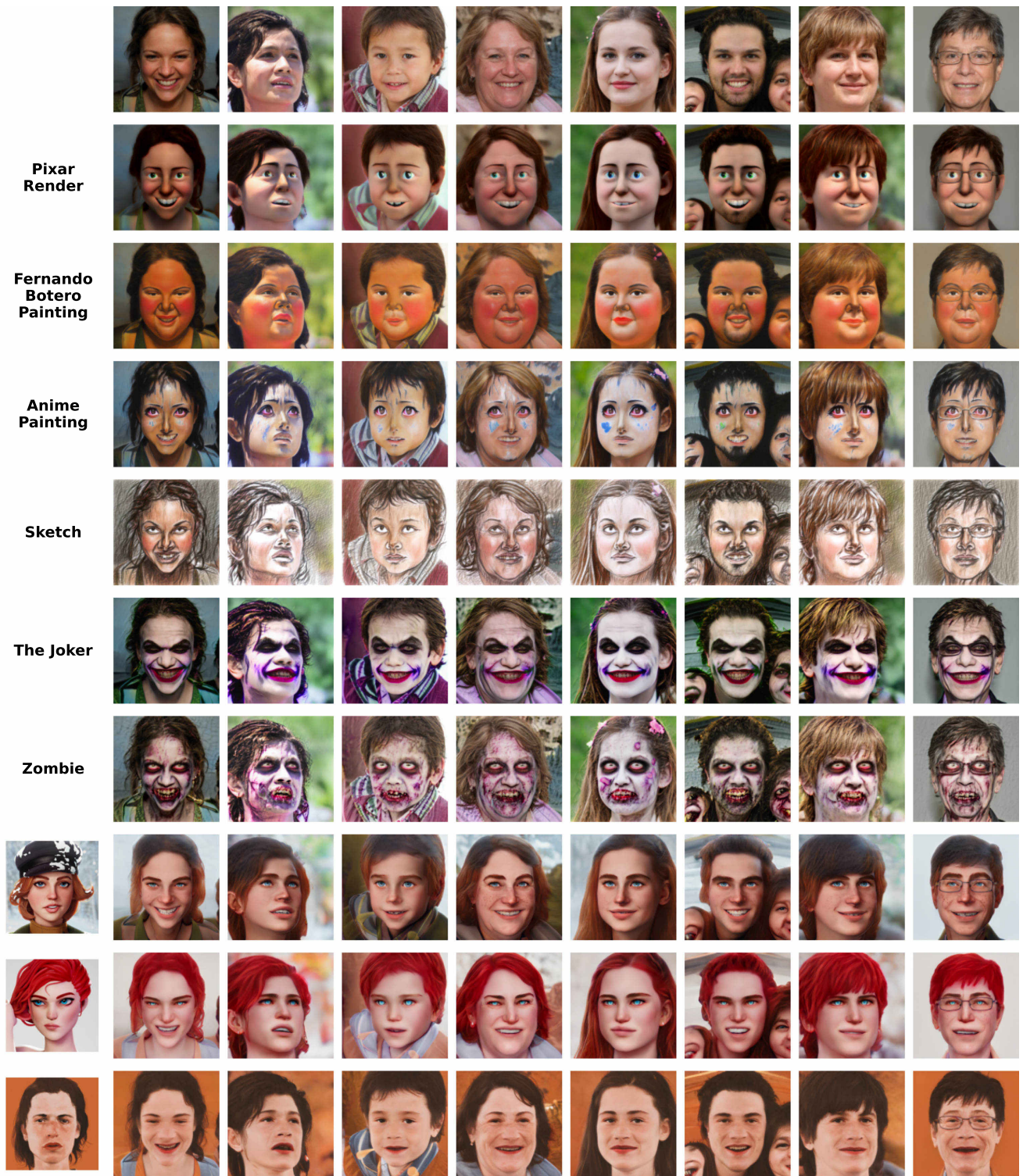


Figure 15. Text-based and one-shot image-based domain adaptation for SyntConv parameterization. Uncurated random samples for each domain.



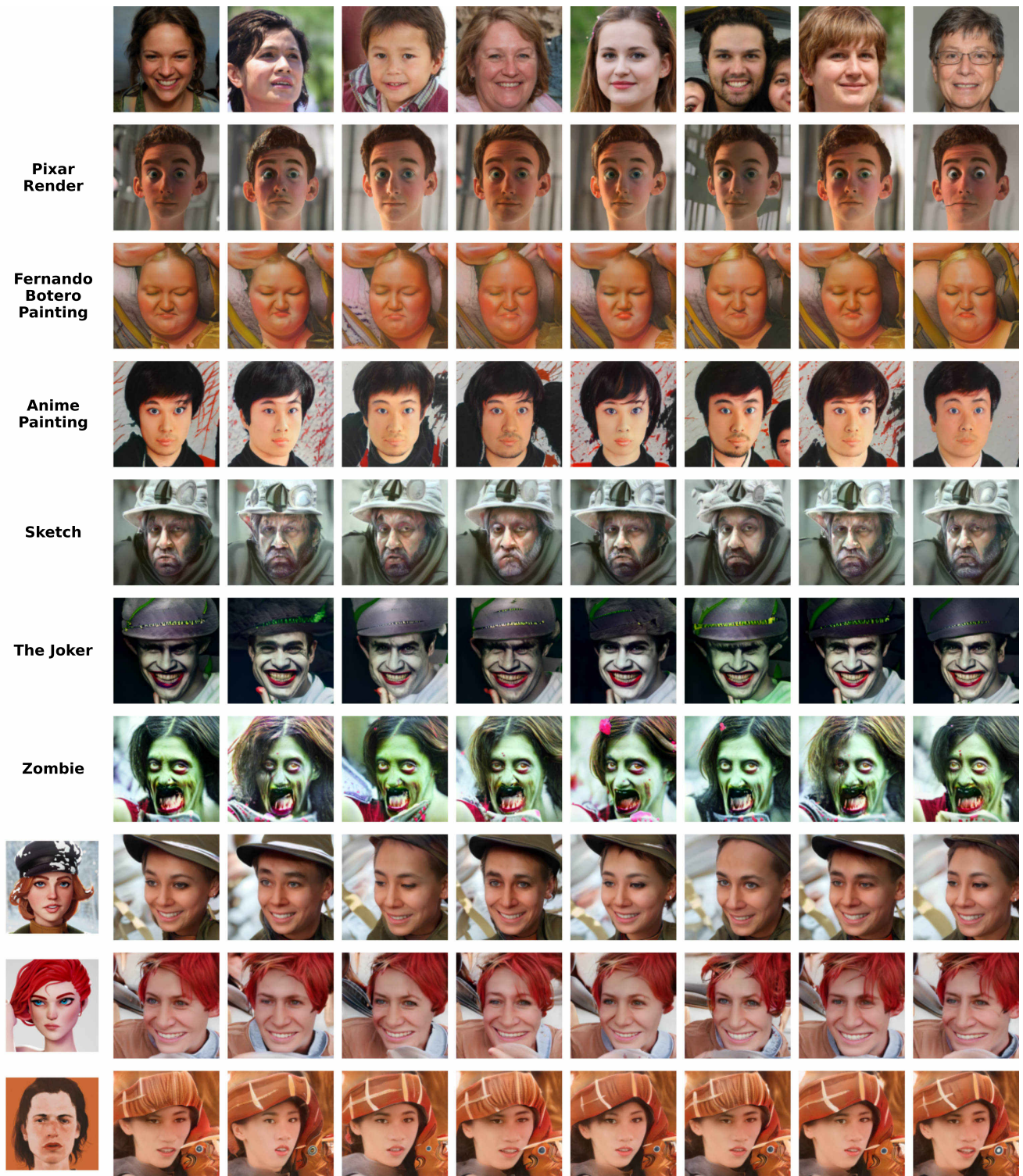


Figure 16. Text-based and one-shot image-based domain adaptation for Mapping parameterization. Uncurated random samples for each domain.

### A.3. Analysis for Moderately Similar and Dissimilar Domains

#### A.3.1 Implementation Details

We use a modified version of the StyleGAN2-ADA Pytorch implementation<sup>3</sup> for training all experiments with moderately similar and dissimilar domains. We downscale images from Metfaces, Mega, Ukiyo-e and Flowers datasets to match  $512 \times 512$  resolution and upscale LSUN Car and Church datasets to the same resolution. Also, we use only 10K random subsets from LSUN Car and LSUN Church datasets and 1K random subset from Flowers dataset. We attach all source code that reproduces our experiments for the setting with moderately similar and dissimilar domains as a part of the supplementary material named "adaptation\_to\_moderately\_similar\_and\_dissimilar\_domains".

#### A.3.2 Hyperparameters

We fine-tune all models to a child domain from the FFHQ512 checkpoint. Specifically, we use model config-f and the default hyper-parameters for `stylegan2` config, except learning rate, from the official Nvidia StyleGAN2-ADA Pytorch implementation. For the Affine+ (and for all models in Table 8), StyleSpace and StyleSpace+ parameterizations, we increase the generator learning rate from 0.002 to 0.02. For other parameterizations, we leave the learning rate unchanged. Also, we use `bgc` augmentation for all domains and parameterizations. We train models on a single Nvidia V100 GPU for 241K images, but for Mega and Ukiyo-e datasets we use intermediate checkpoints with 40K and 100K images respectfully.

#### A.3.3 Quantitative Results

For quantitative comparison, we compute FID5k (denoted as FID) using 5000 generated images and all training images. We also compute FID50k and KID50k (denoted as KID) using 50000 generated images and all training images. These metrics in Tables [6, 7] reaffirm our observation that the Affine+ parameterization can close the gap with the Full parameterization for most of the domains. For the Car domain, the quality gap remains, although ten times less than for the Affine parameterization.

Table 6. FID50k scores for moderately similar and dissimilar domains. Affine+ has results comparable to the Full or SyntConv parameterizations for all domains except Car dataset.

Parameter Space	Size	Metfaces	Mega	Ukiyoe	Dog	Cat	Car	Church	Flowers
Full	30.3M	20.0	80.4	19.6	18.9	5.9	20.9	15.0	14.8
SyntConv	23.6M	21.5	81.5	21.2	20.0	6.1	22.6	15.4	15.0
Affine+	5.1M	20.2	77.2	24.0	17.1	5.6	38.2	16.2	15.6
Affine	4.6M	24.3	107.9	60.3	68.0	27.0	110.4	85.9	40.4
Mapping	2.1M	53.4	136.2	155.6	206.2	225.6	237.1	263.5	234.3

Table 7.  $KID \times 10^3$  metric for moderately similar and dissimilar domains. Affine+ has results comparable to the Full or SyntConv parameterizations for all domains except Car dataset.

Parameter Space	Size	Metfaces	Mega	Ukiyoe	Dog	Cat	Car	Church	Flowers
Full	30.3M	2.6	12.8	11.5	9.1	1.8	7.8	7.8	4.6
SyntConv	23.6M	3.4	13.2	13.5	10.7	1.7	9.8	7.2	4.9
Affine+	5.1M	3.5	14.1	16.3	7.8	1.2	16.3	7.8	4.2
Affine	4.6M	4.5	28.8	52.8	56.0	17.7	88.0	77.2	24.2
Mapping	2.1M	22.6	52.7	161.9	169.4	223.2	240.3	298.5	224.2

Exact Affine+ parameterization was selected by analyzing three different domains: Metfaces, Dog and Church. Table 8 demonstrates that Affine+64 has the best performance on these datasets and therefore is selected for the further analysis.

<sup>3</sup><https://github.com/NVLabs/stylegan2-ada-pytorch>



Table 8. Comparison of different block resolutions for the Affine+ parameterization. Affine+64 shows the best performance for the moderately similar and for the distant domains. It is denoted as Affine+ parameterization for the rest of the text.

Dataset	Affine+4	Affine+8	Affine+16	Affine+32	Affine+64	Affine+128	Affine+256	Affine+512
Size	4.9M	5.1M	5.1M	5.1M	5.1M	4.8M	4.6M	4.6M
Metfaces	22.8	23.0	<b>22.0</b>	22.5	<b>22.1</b>	23.0	23.2	23.2
Dog	24.9	24.3	21.6	19.5	<b>18.6</b>	18.9	21.8	25.7
Church	23.2	23.4	22.3	20.5	<b>18.8</b>	20.1	21.3	22.7

### A.3.4 Qualitative Results

In this section, we provide generated images for all datasets (Metfaces, Mega, Ukiyo-e, Dog, Cat, Car, Church and Flowers) alongside with uncurated results for parameterizations and datasets.

Figures [17, 18] show that Affine+ parameterization has comparable visual quality and diversity with Full and SyntConv parameterizations for all domains (including dissimilar ones) while having less trainable parameters by the factor of five. At the same time, Affine or Mapping parameterizations fail even on moderately similar domains (Cat, Dog).

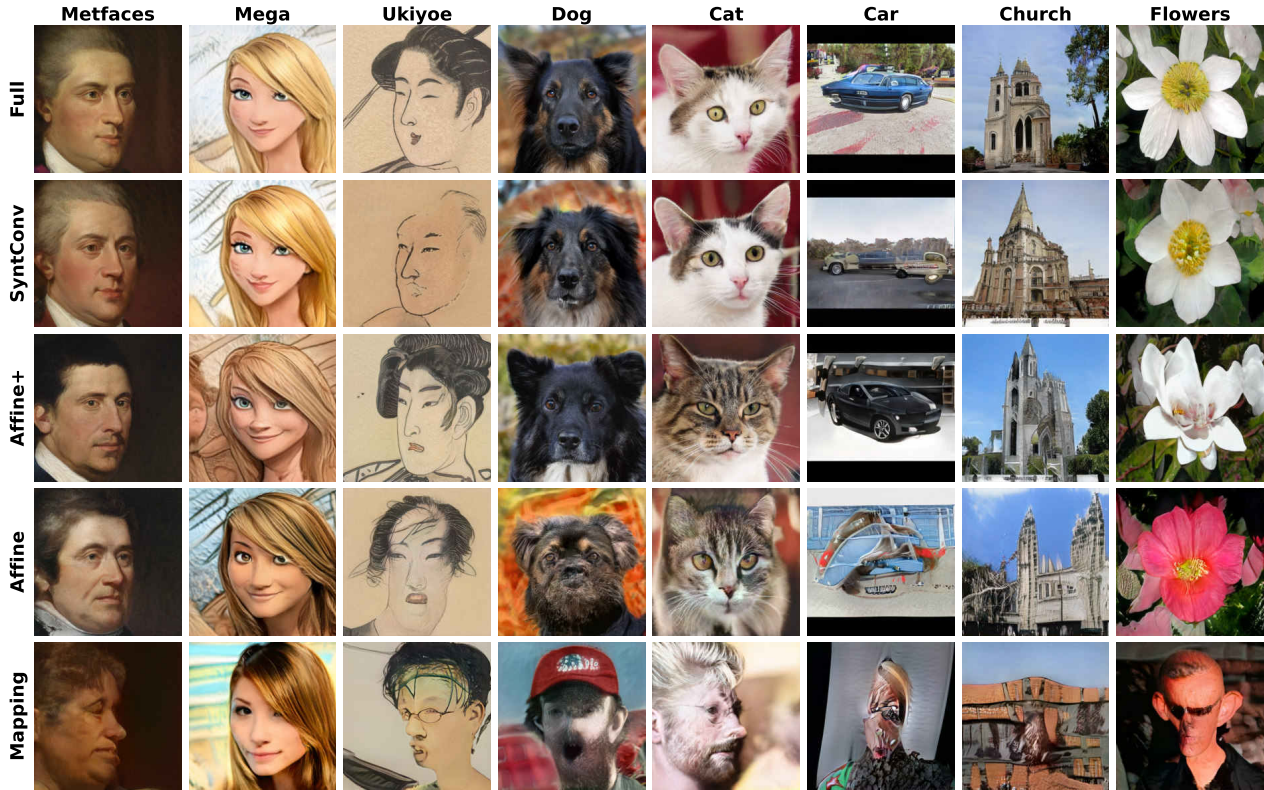


Figure 17. Domain adaptation for moderately similar and dissimilar domains. Affine+ parameterization produce results on par with Full one even for dissimilar domains (Cat, Church).





Figure 18. Domain adaptation for moderately similar and dissimilar domains. Uncurated results for each dataset and generator.

## A.4. StyleSpace Results

### A.4.1 Analysis for Similar Domains

We provide more results on capabilities of StyleDomain directions for the case of similar domains. At first, we evaluate StyleSpace parameterization for a large number of different domains in Table 1. We see that for all considered domains StyleDomain directions achieve results comparable to the Full parameterization in terms of both Quality and Diversity metric. It shows that StyleSpace allows us to successfully adapt the whole generator to similar domains. Qualitative results in Figures 19 to 21 confirm our conclusions.



Figure 19. Text-based and one-shot image-based domain adaptation for different parameterizations. StyleSpace achieves visual quality on par with Full parameterization.

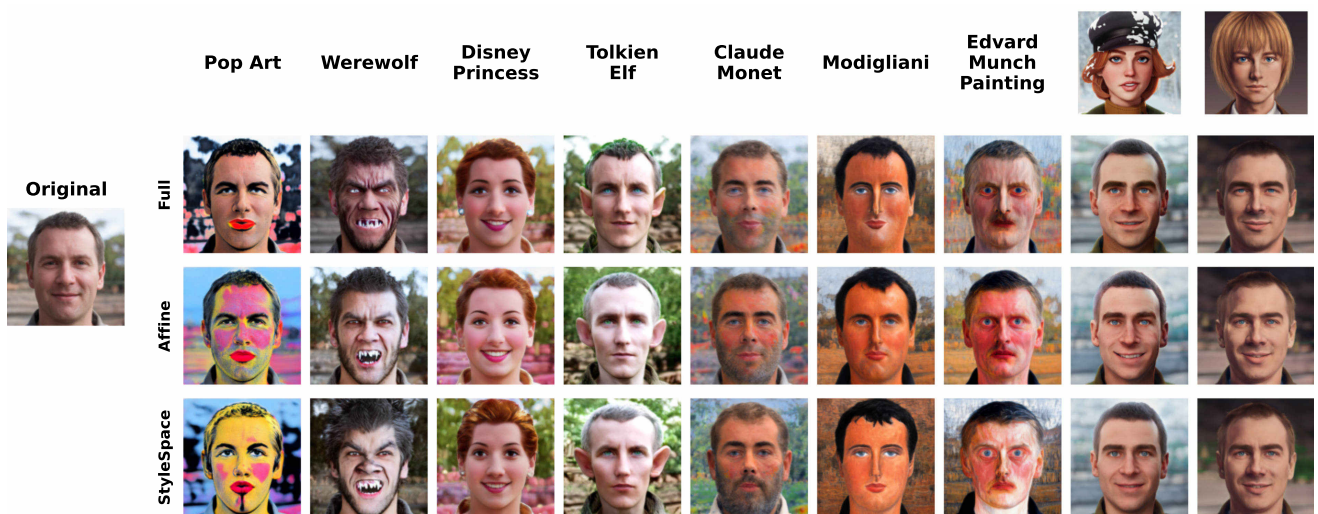


Figure 20. Text-based and one-shot image-based domain adaptation for different parameterizations. StyleSpace achieves visual quality on par with Full parameterization.

Table 9. Quality and Diversity metrics [4] for text-based and one-shot image-based domain adaptation. StyleSpace parameterization achieves comparable results as Full parameterization.

	Quality		Diversity	
	Full	StyleSpace	Full	StyleSpace
<b>Text Domains</b>				
Anime Painting	0.25	0.27	0.25	0.22
Pixar Render	0.27	0.26	0.21	0.22
Sketch	0.21	0.19	0.30	0.32
Ukiyo-e Painting	0.22	0.22	0.22	0.22
Fernando Botero Painting	0.31	0.30	0.23	0.22
Pop Art	0.25	0.25	0.27	0.29
Werewolf	0.26	0.25	0.13	0.16
Zombie	0.24	0.24	0.12	0.15
The Joker	0.25	0.24	0.17	0.20
Disney Princess	0.23	0.22	0.24	0.27
Cubism	0.23	0.22	0.22	0.24
Tolkien Elf	0.27	0.28	0.22	0.21
Impressionism	0.27	0.25	0.25	0.28
Claude Monet	0.21	0.20	0.24	0.32
Modigliani	0.27	0.26	0.20	0.22
The Thanos	0.23	0.25	0.29	0.28
Edvard Munch Painting	0.25	0.24	0.20	0.20
Dali Painting	0.26	0.24	0.22	0.21
<b>Image Domains</b>				
Anastasia	0.64	0.61	0.28	0.30
Mermaid	0.64	0.63	0.26	0.26
Titan Erwin	0.65	0.64	0.28	0.28
Titan Armin	0.58	0.58	0.29	0.30
Speed Paint	0.65	0.63	0.31	0.32



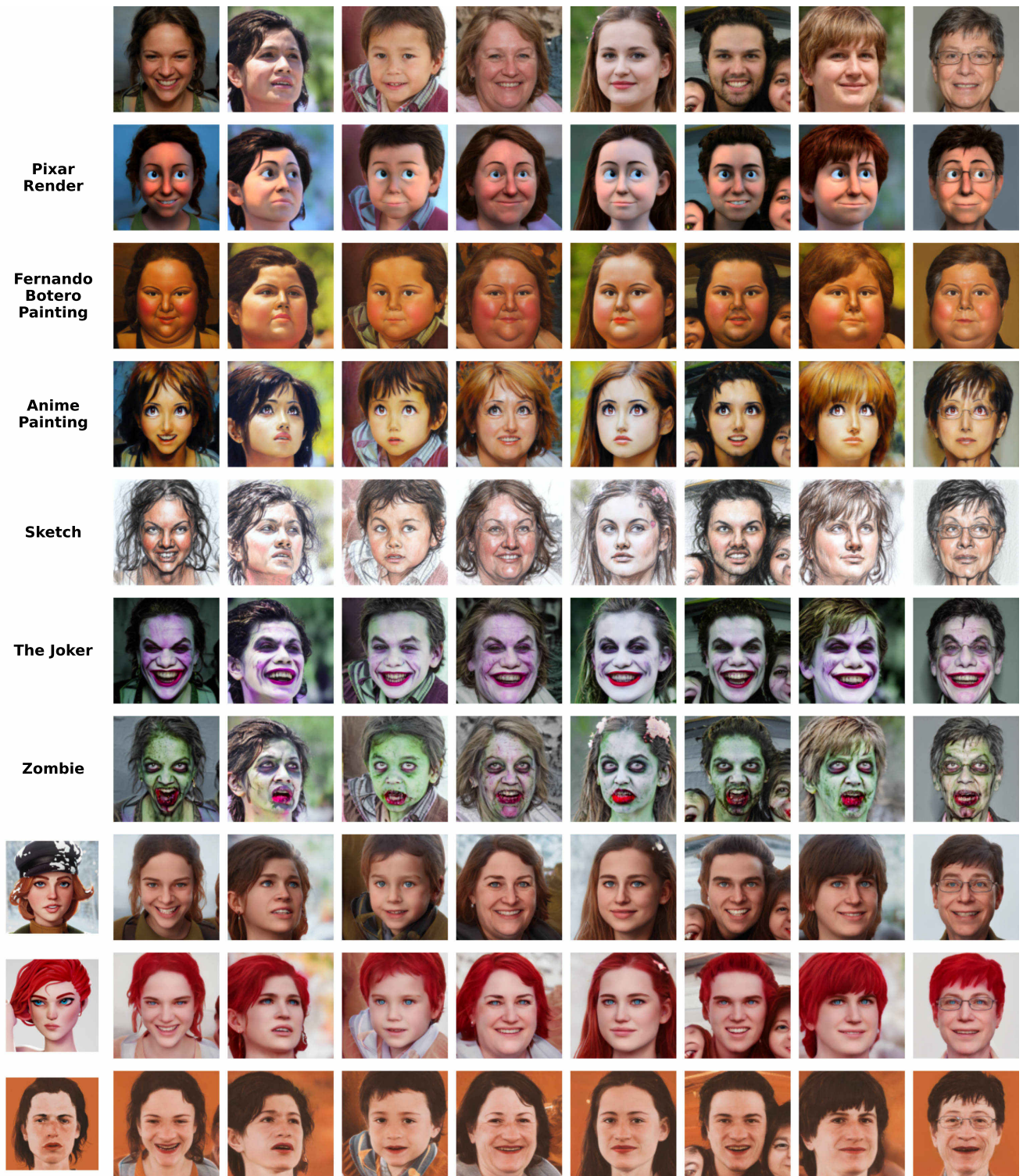


Figure 21. Text-based and one-shot image-based domain adaptation for StyleSpace parameterization. Uncurated random samples for each domain.



### A.4.2 Analysis for Moderately Similar and Dissimilar Domains

We provide additional results for the StyleSpace and StyleSpace+ parameterizations for the cases of moderately similar and dissimilar domains.

We report FID50k and KID50k scores in Tables [10, 11]. It can be seen that the results are similar to Table 3, where the StyleSpace works much worse than the Full parameterization, but adding weight offsets can improve quality for all datasets. So, StyleSpace+ parameterization achieves comparable scores for the moderately similar domains as the Full parameterization while having 60 times less parameters. For dissimilar domains the gap is larger, but it is much less than for StyleSpace parameterization. Figures [18, 22] show that StyleSpace+ parameterization can generate good quality samples even for dissimilar domains. On the other hand, StyleSpace parameterization works well only for the most similar domains, like Metfaces and Ukiyo-e.

Table 10. FID50k scores for domain adaptation in  $S$  and  $S+$ .  $S+$  parameterization can be competitive for moderately similar domains

Parameter Space	Size	Metfaces	Mega	Ukiyoe	Dog	Cat	Car	Church	Flowers
Full	30.3M	20.0	80.4	19.6	18.9	5.9	20.9	15.0	14.8
Affine+	5.1M	20.2	77.2	24.0	17.1	5.6	38.2	16.2	15.6
StyleSpace+	0.5M	23.5	82.5	29.1	28.0	7.8	41.7	25.7	19.9
StyleSpace	9.0K	28.6	102.0	48.8	74.2	20.6	132.3	63.9	36.8

Table 11.  $KID \times 10^3$  scores for domain adaptation in  $S$  and  $S+$ .  $S+$  parameterization can be competitive for moderately similar domains

Parameter Space	Size	Metfaces	Mega	Ukiyoe	Dog	Cat	Car	Church	Flowers
Full	30.3M	2.6	12.8	11.5	9.1	1.8	7.8	7.8	4.6
Affine+	5.1M	3.5	14.1	16.3	7.8	1.2	16.3	7.8	4.2
StyleSpace+	0.5M	5.2	16.1	21.3	16.4	2.4	21.8	14.4	8.8
StyleSpace	9.0K	6.5	24.6	41.8	65.7	11.6	132.6	55.6	21.6

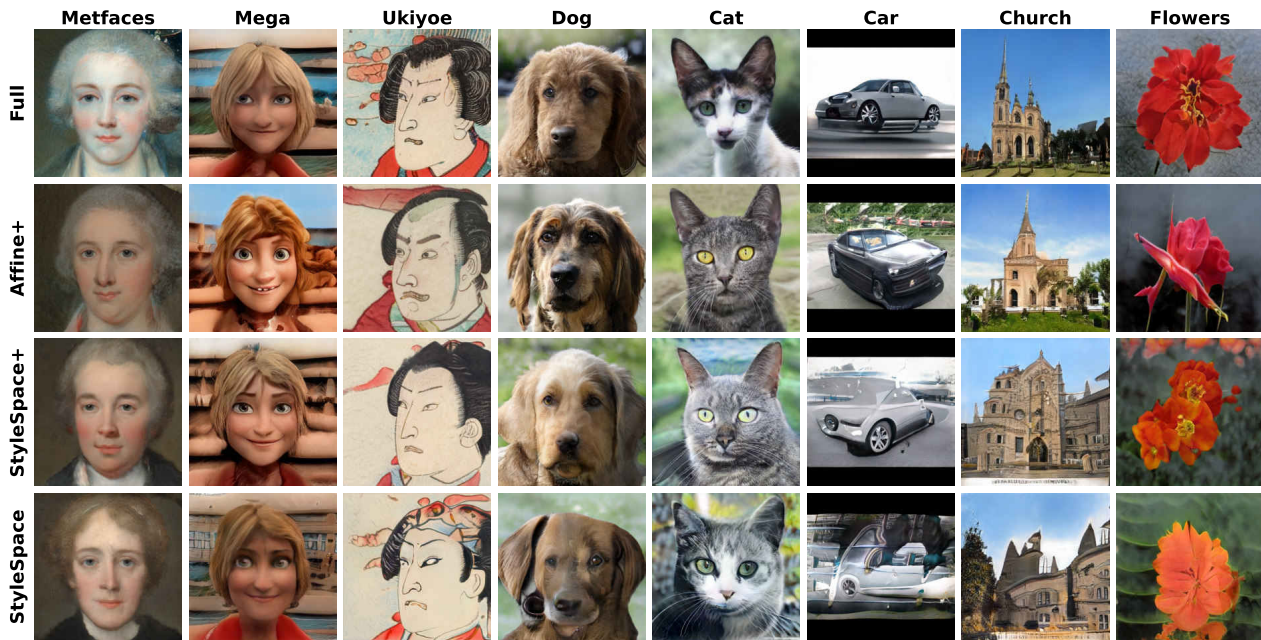


Figure 22. Domain adaptation for moderately similar and dissimilar domains. StyleSpace+ parameterization closes the gap in quality for all presented domains despite having 60 times less trainable parameters.

## A.5. Properties of StyleDomain Directions

### A.5.1 Transferability of StyleDomain Directions to Other Aligned StyleGAN Models

**StyleDomain directions of similar domains.** We illustrate the ability of StyleDomain directions optimized for the base generator (e.g. pretrained on FFHQ) to be transferable to other aligned generators fine-tuned to other domains (e.g. MetFaces, Mega, Dogs, etc.). We apply StyleDomain directions that correspond to a wide range of text-based and image-based domains to different aligned generators in Figures 23 and 24. We observe that transferability is successful for moderately similar domains and reasonable for dissimilar domains.

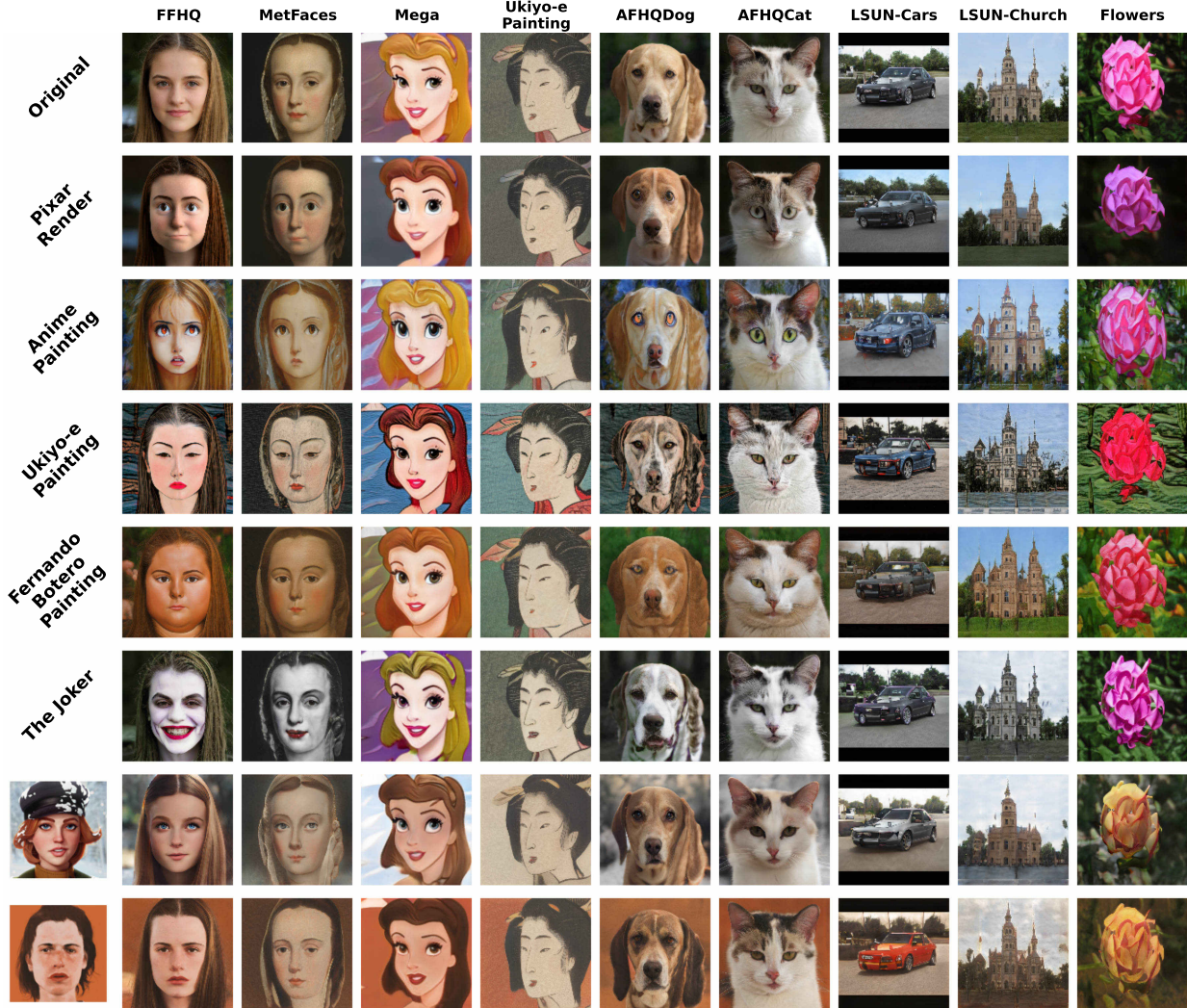


Figure 23. Examples of transferability of StyleDomain directions optimized for similar domains (text-based and one-shot image-based) to aligned generators fine-tuned to other domains (MetFaces, Mega, Dog, etc.). We observe successful transferability for moderately similar domains and reasonable quality for dissimilar ones.



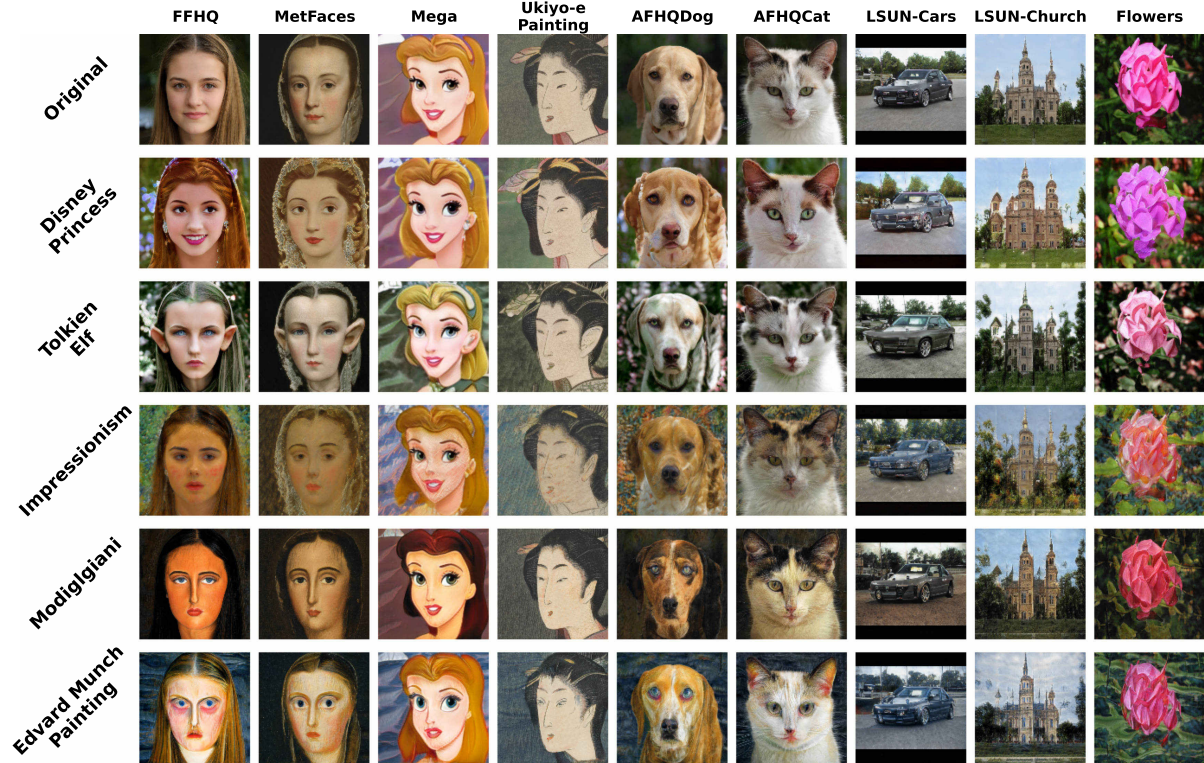


Figure 24. Examples of transferability of StyleDomain directions optimized for similar domains (text-based and one-shot image-based) to aligned generators fine-tuned to other domains (MetFaces, Mega, Dog, etc.). We observe successful transferability for moderately similar domains and reasonable quality for dissimilar ones.

**StyleDomain directions of moderately similar domains.** We illustrate the ability of StyleDomain directions from the fine-tuned models to be transferable to the other aligned generators. We apply these directions from the StyleSpace optimized for Metfaces, Mega and Ukiyo-e domains to the generators that fine-tuned to the moderately similar and dissimilar domains in the Full parameterization.

From Figures [25, 26] we observe that StyleDomain directions can be used to change the style of generated images. Such model modifications work for the moderately similar (most prominently Dog) and for some dissimilar domains (Flowers).

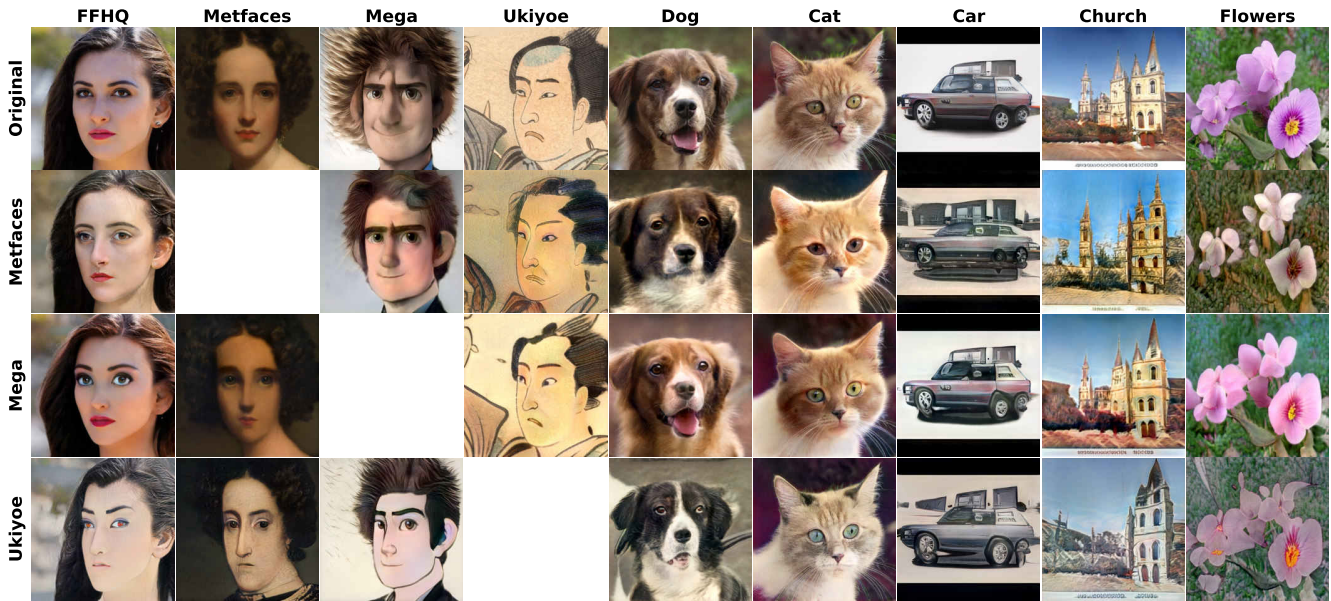


Figure 25. Examples of transferability of StyleDomain directions optimized for moderately similar domains (MetFaces, Mega, Ukiyo-e) to aligned generators fine-tuned to other domains (MetFaces, Mega, Dog, etc.). We observe successful transferability for moderately similar domains and reasonable quality for dissimilar ones.

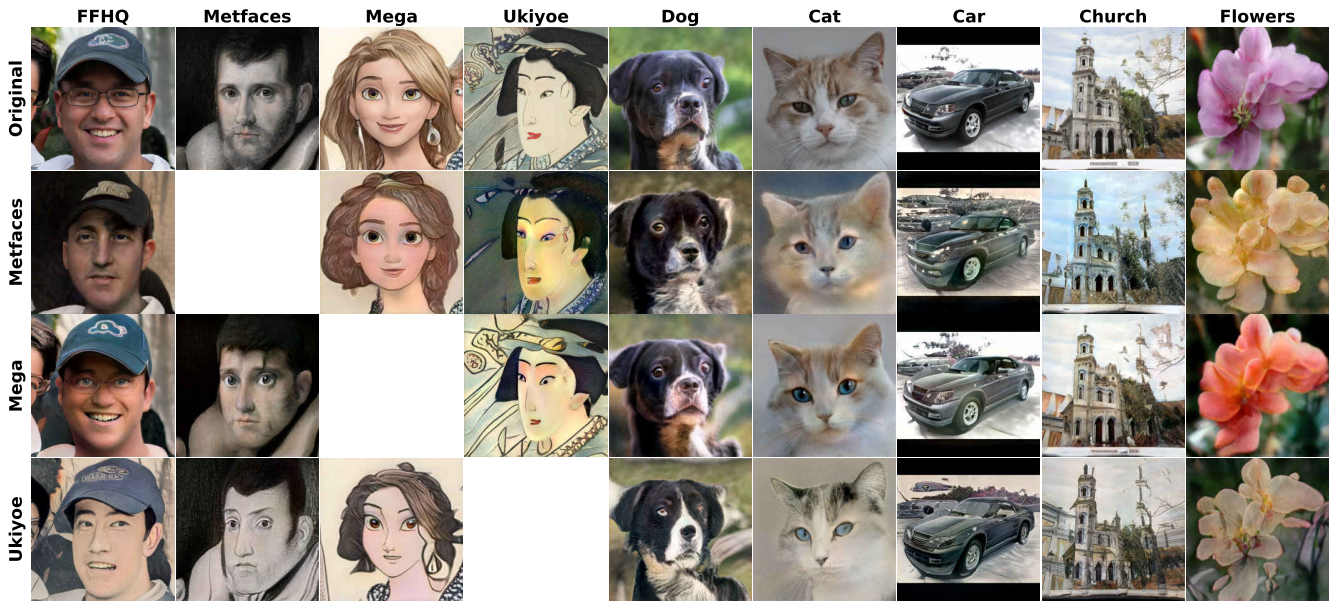


Figure 26. Examples of transferability of StyleDomain directions optimized for moderately similar domains (MetFaces, Mega, Ukiyo-e) to aligned generators fine-tuned to other domains (MetFaces, Mega, Dog, etc.). We observe successful transferability for moderately similar domains and reasonable quality for dissimilar ones.

### A.5.2 Combinations of StyleDomain Directions for Mixed Domain Adaptation

We present more examples of the StyleDomain directions property to be combined with each other to obtain new mixed domains. In Figures 27 and 28 we consider all pairwise combinations between different text-based and image-based domains. We observe that new obtained mixed domains have meaningful semantic blending of the corresponding two domains. We also consider combinations of three different domains and provide several examples in Figure 29. We see that these mixed domains also have a recognisable semantic sense.



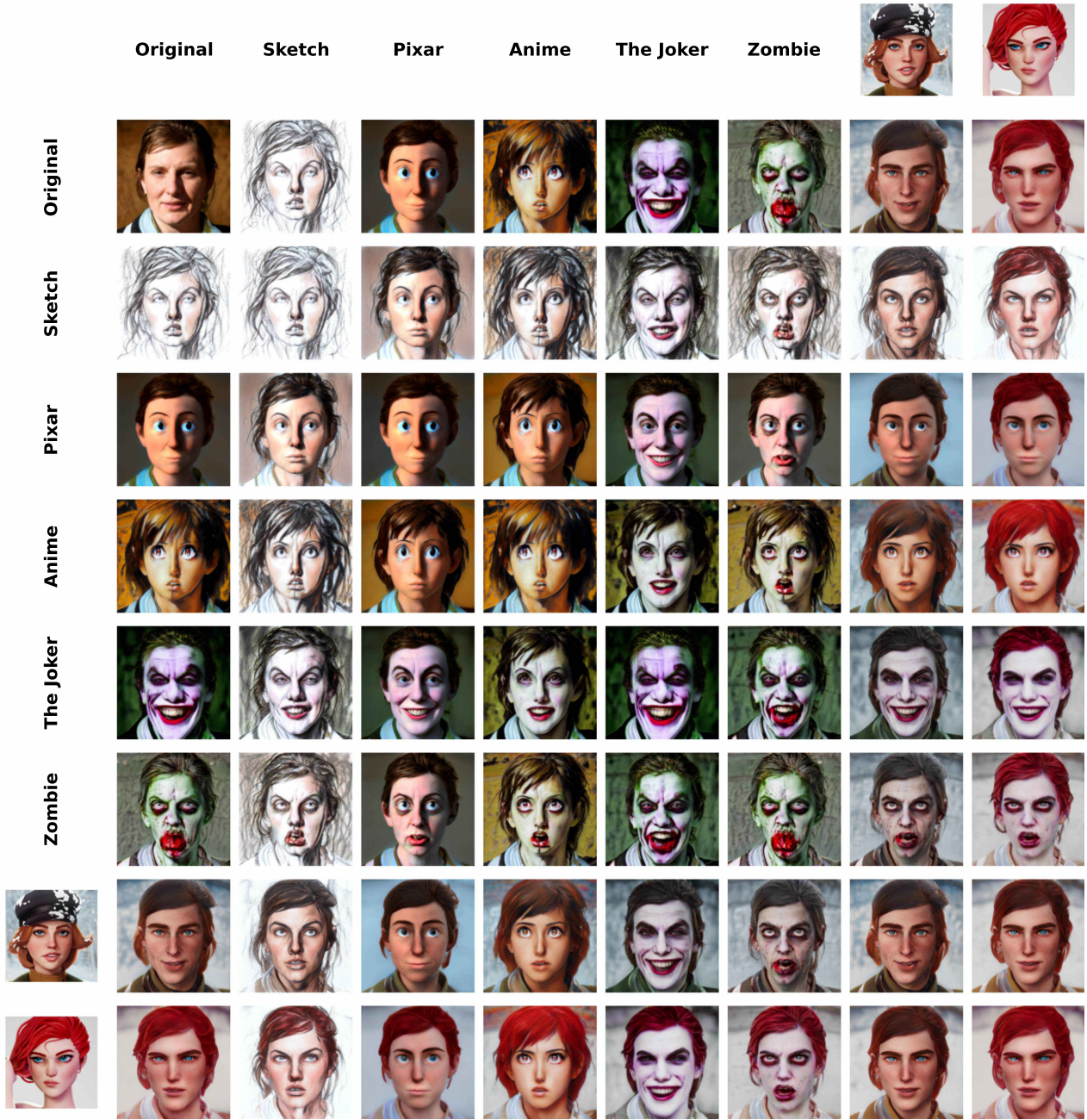


Figure 27. Pairwise combinations of different StyleDomain directions that correspond to text-based or image-based domains. We observe semantically meaningful mixed domains.



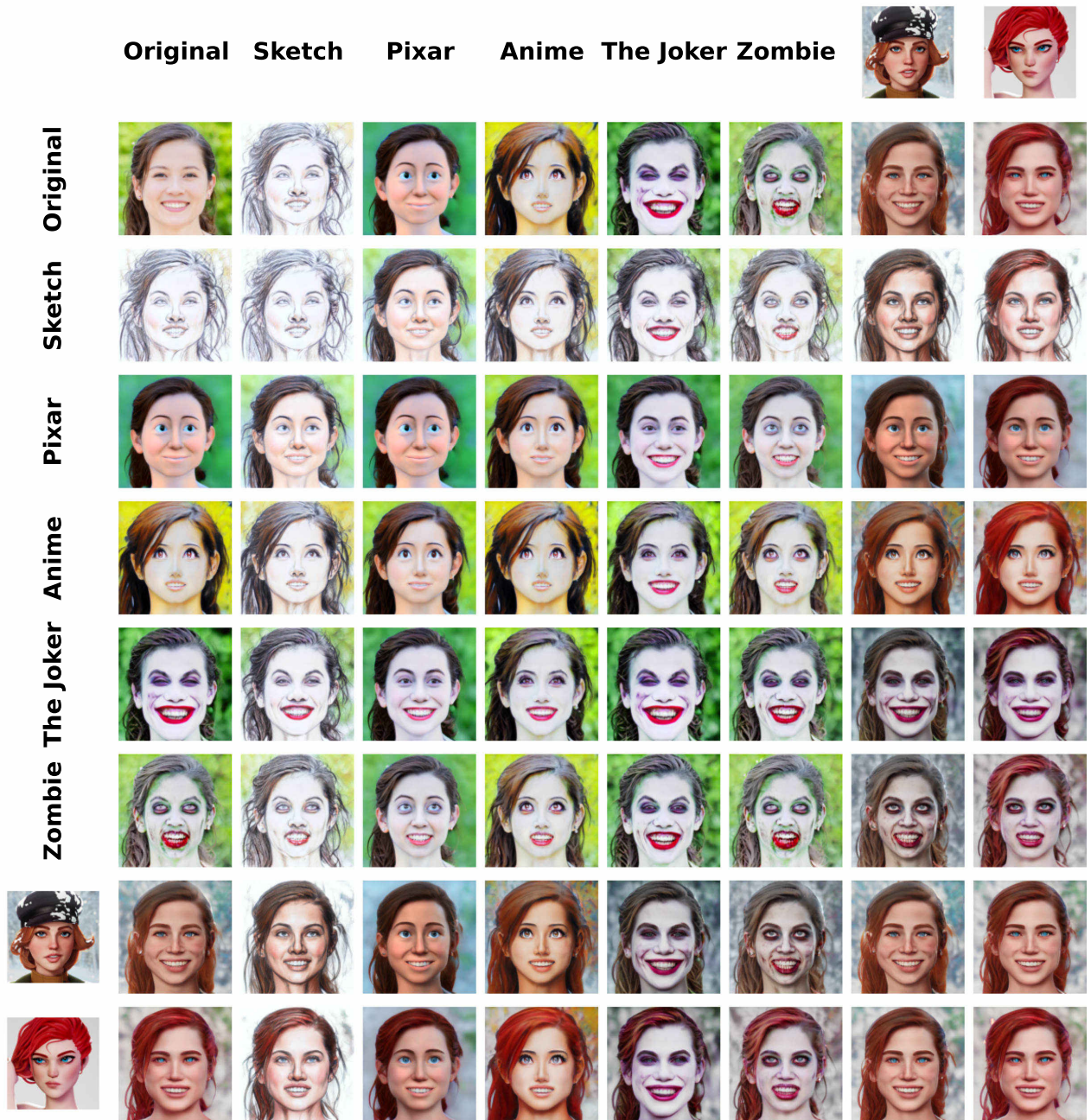


Figure 28. Pairwise combinations of different StyleDomain directions that correspond to text-based or image-based domains. We observe semantically meaningful mixed domains.

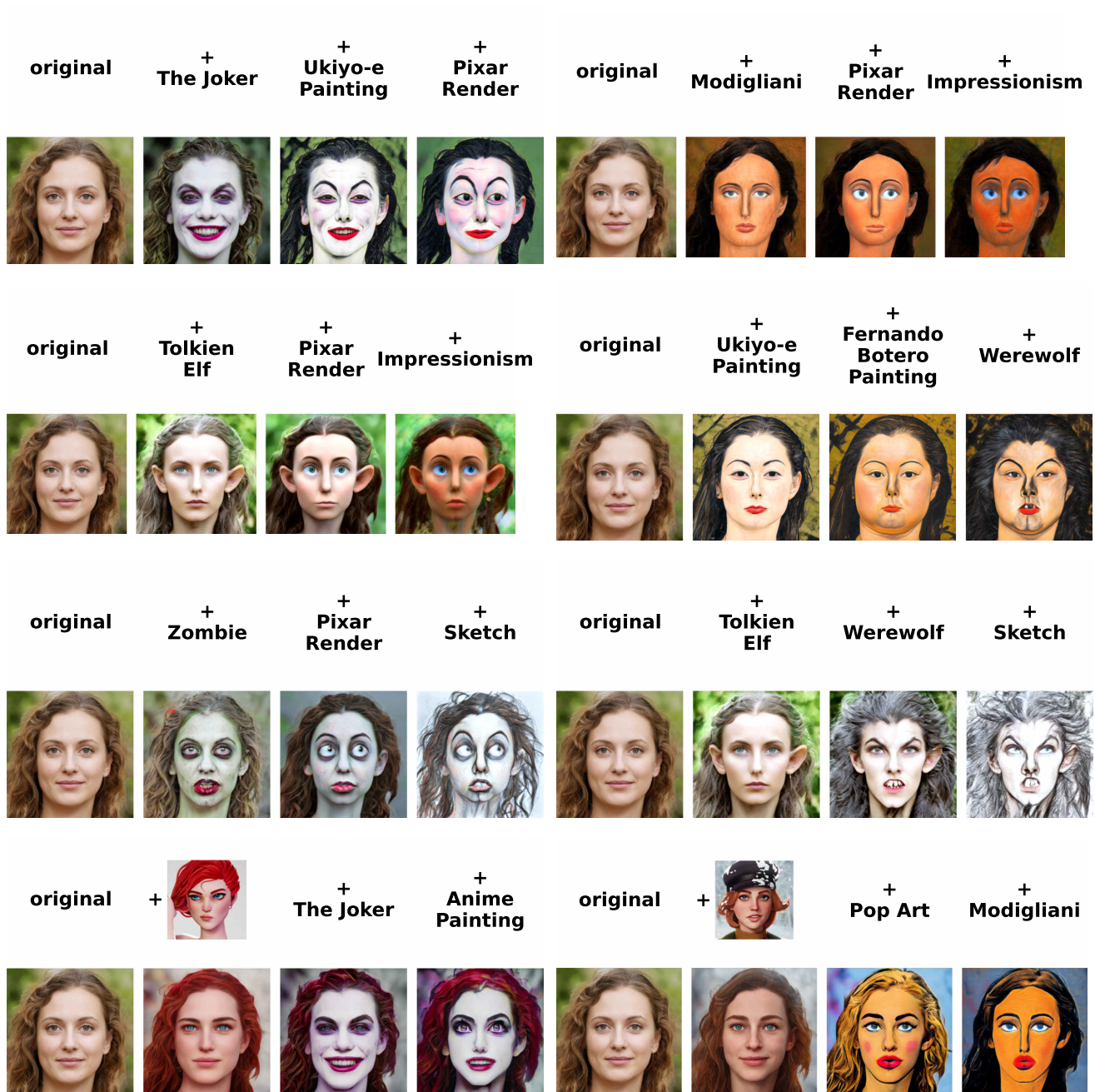


Figure 29. Triple combinations of different StyleDomain directions that correspond to text-based or image-based domains. We observe semantically meaningful mixed domains.



### A.5.3 Semantic Editing for Similar Domains

We demonstrate how StyleDomain directions can be combined with latent transformations for semantic editing.

We utilize the StyleSpace [41] editing method for "Black hair", "Smile" and "Lipstick" attributes. InterFaceGan [33] editing method is used for "Yaw", "Rejuvenation", "Aging", "Gender".

Figures 30 and 31 show results of combination of StyleDomain directions for different text-based and image-based domains and editing of mentioned attributes. We see that domain and modification directions are orthogonal, so they are combined successfully.

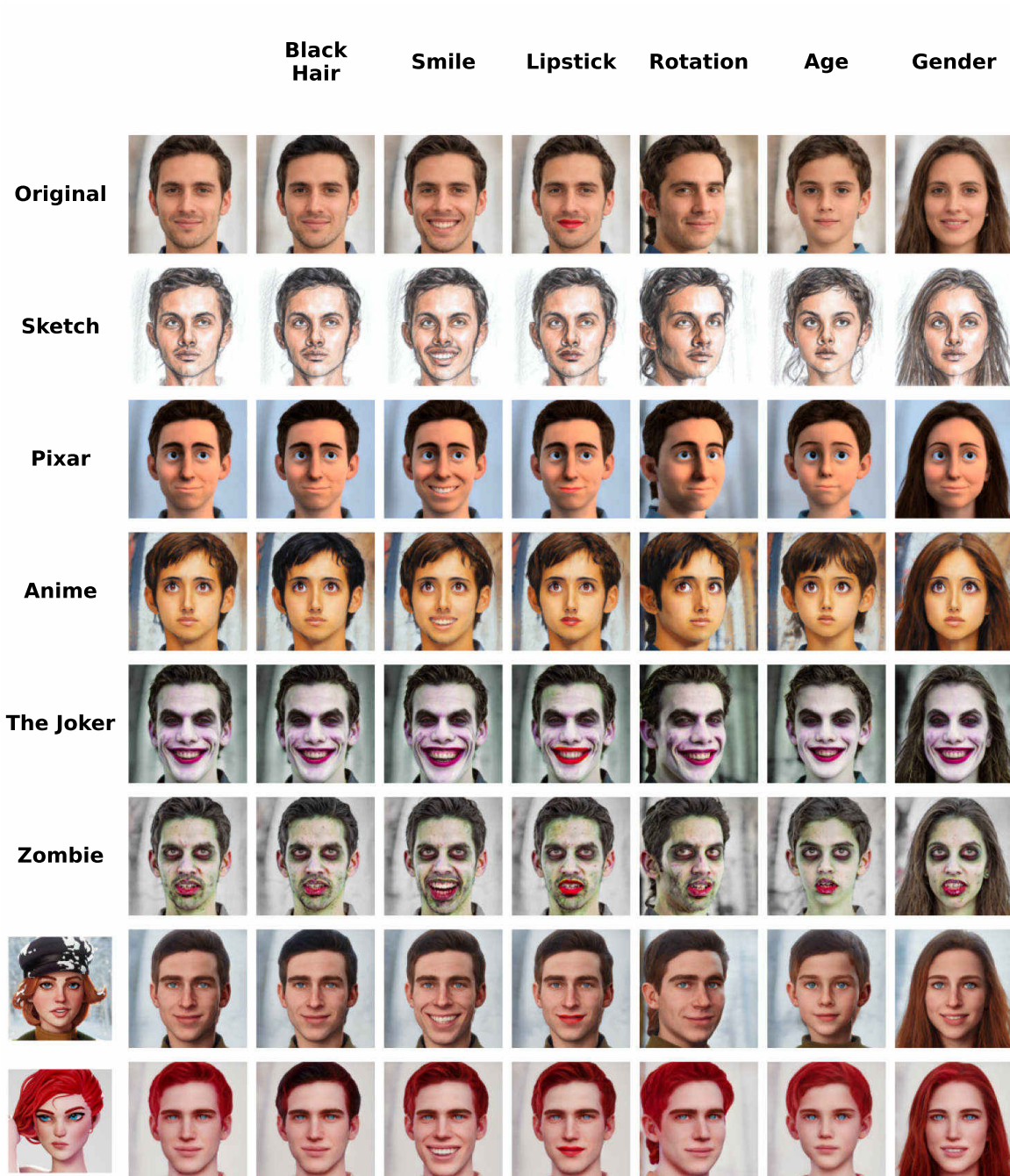


Figure 30. Combination of StyleDomain directions with semantic editing. We observe that they are successfully combined.

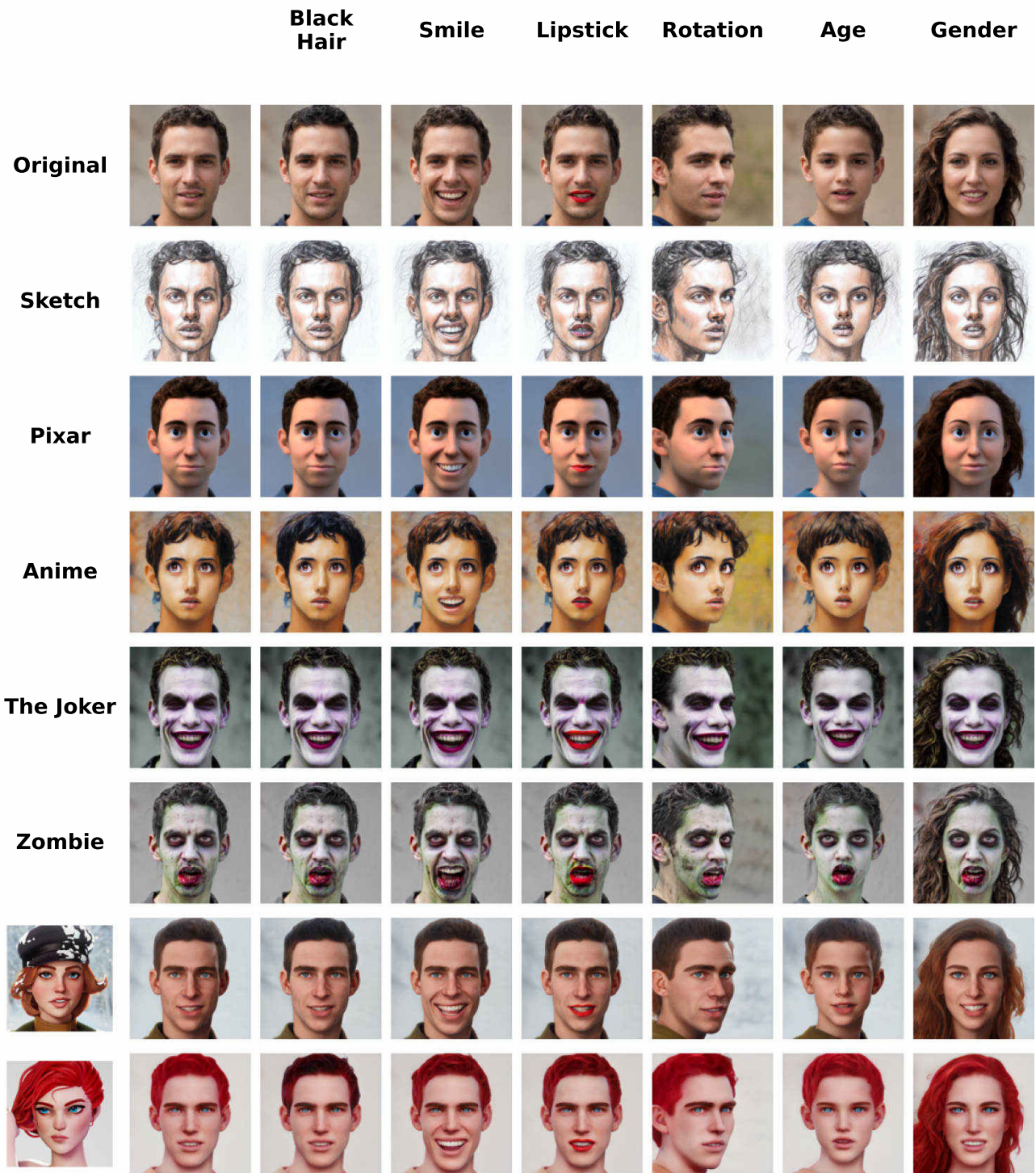


Figure 31. Combination of StyleDomain directions with semantic editing. We observe that they are successfully combined.

#### A.5.4 Semantic Editing for Moderately Similar and Dissimilar Domains

We analyze the ability to be semantically edited for different parameterizations in the case of moderately similar and dissimilar domains.



We use the StyleSpace [41] editing method for "Blond Hair", "Black Hair", "Smile", "Lipstick", "Short Hair", "Wavy Hair" and "Gaze" attributes. The StyleFlow [2] editing method is used for "Yaw", "Rejuvenation", "Aging", "Gender". Since the models for modifications imply using of images in  $1024 \times 1024$  resolution, we train separate models in this resolution from FFHQ1024 checkpoint. We use exactly the same setup as described in Appendix A.3 for training these models.

As can be seen from Figure 32, we can utilize existing latent transformations for models fine-tuned with different parameterizations. Notably, we can successfully apply simple style modifications (change of hair color) as well as complex shape transformations (change in age and gender). For more distant domains in Figures [33, 34, 35] some controls become much less pronounced ("Smile") or even inoperable ("Lipstick").

We observe a negligible difference in the quality of modifications between different parameterizations. So, we can conclude that the ability to perform latent transformations mostly depends on the target dataset rather than the choice of parameterization.

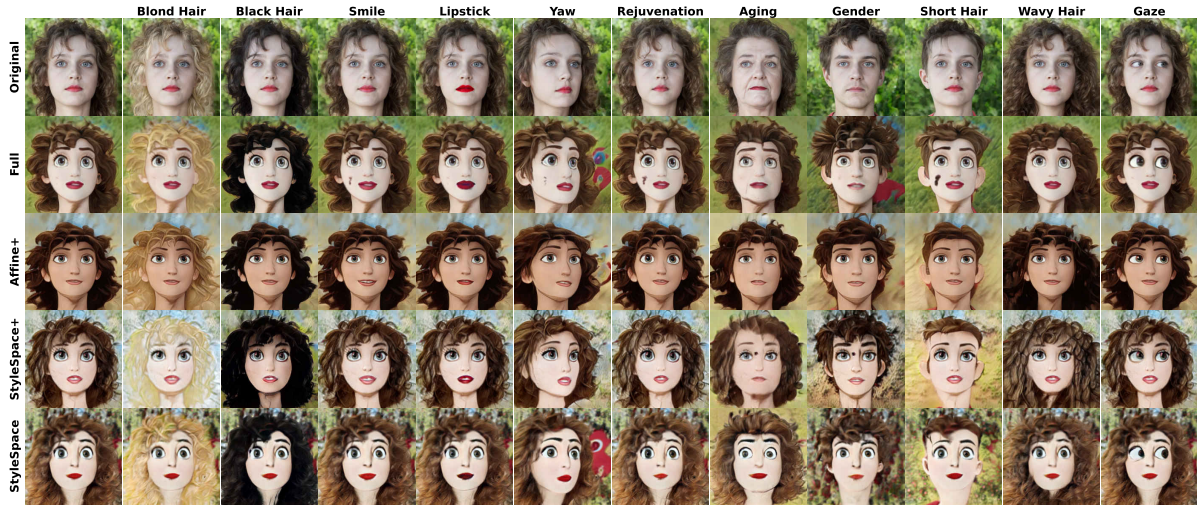


Figure 32. Examples of different parameterizations mixed with semantic editing for Mega. Top row represents attribute names. We can control style (color of hair or lips) as well as the shape (age, gender, hair length and yaw) for all parameterizations.

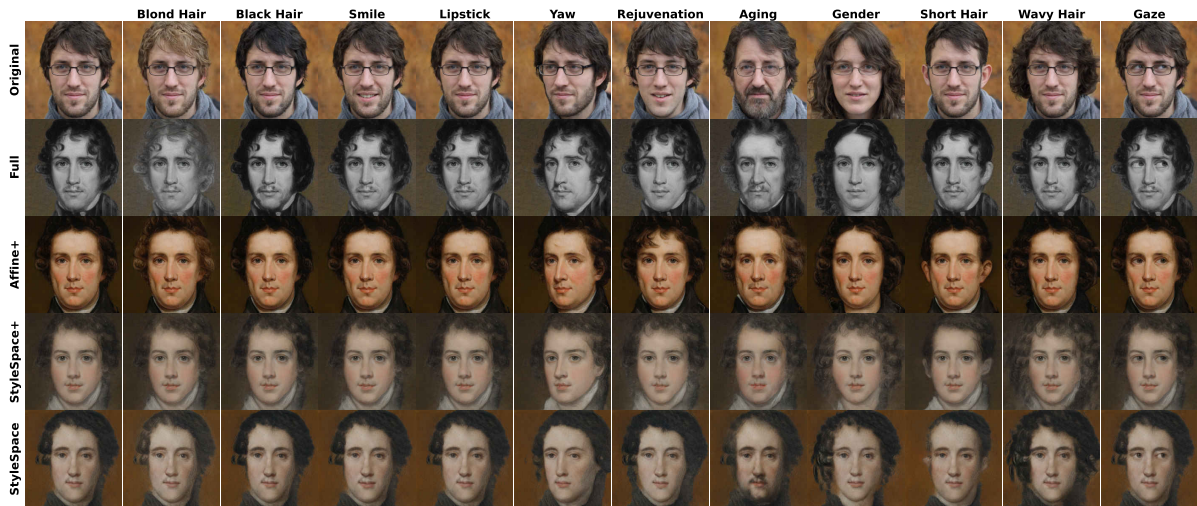


Figure 33. Examples of different parameterizations mixed with semantic editing for Metfaces. Top row represents attribute names.



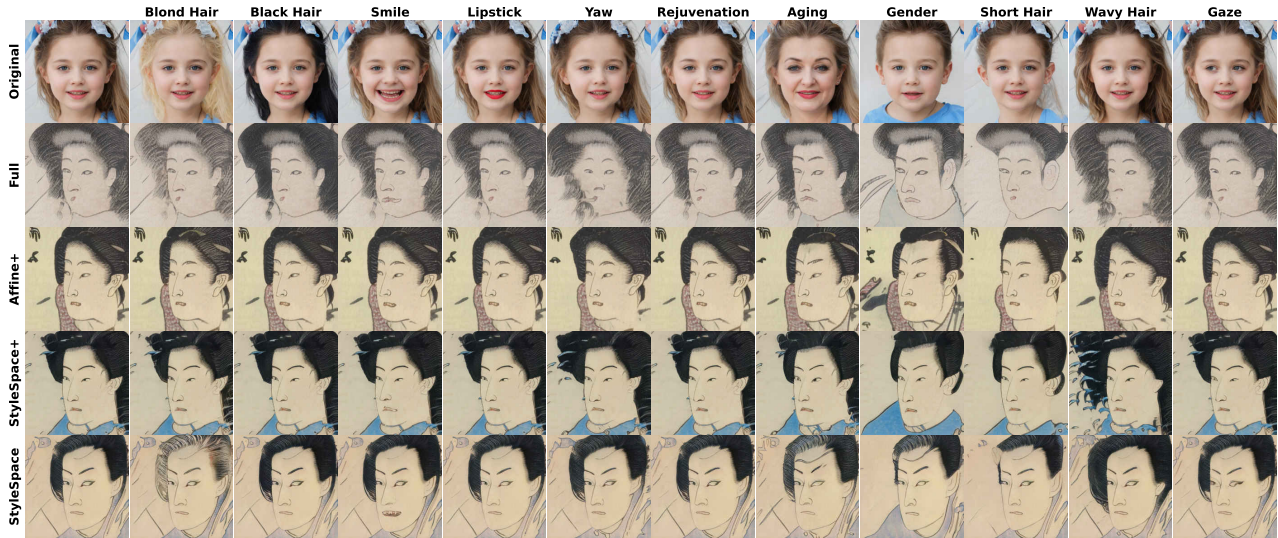


Figure 34. Examples of different parameterizations mixed with semantic editing for Ukiyo-e. Top row represents attribute names. Most of the transformations are inoperable regardless of the exact choice of parameterization.

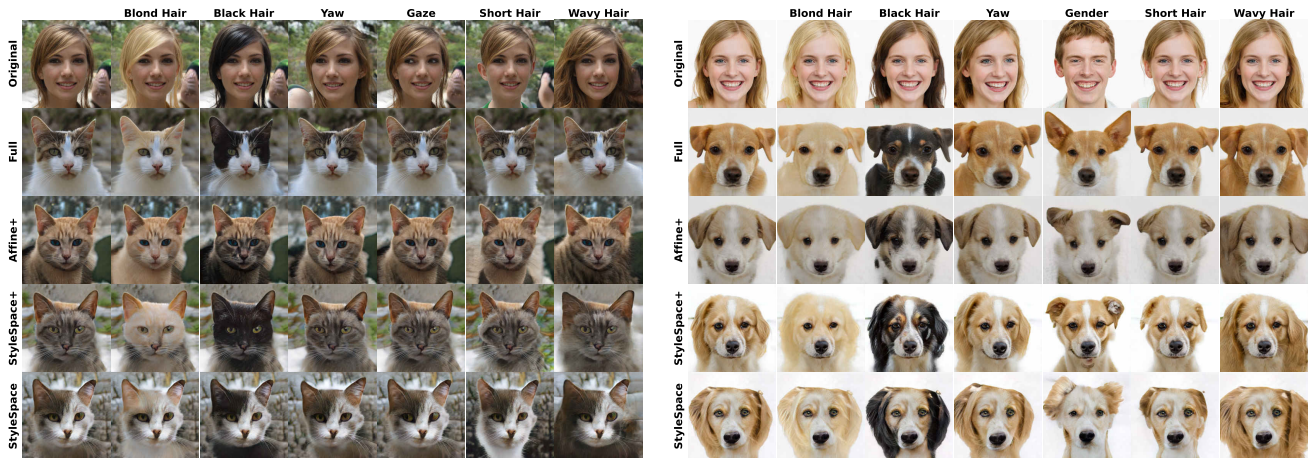


Figure 35. Examples of different parameterizations mixed with semantic editing for Cat and Dog. Top row represents attribute names. Only working latent transformations are left.

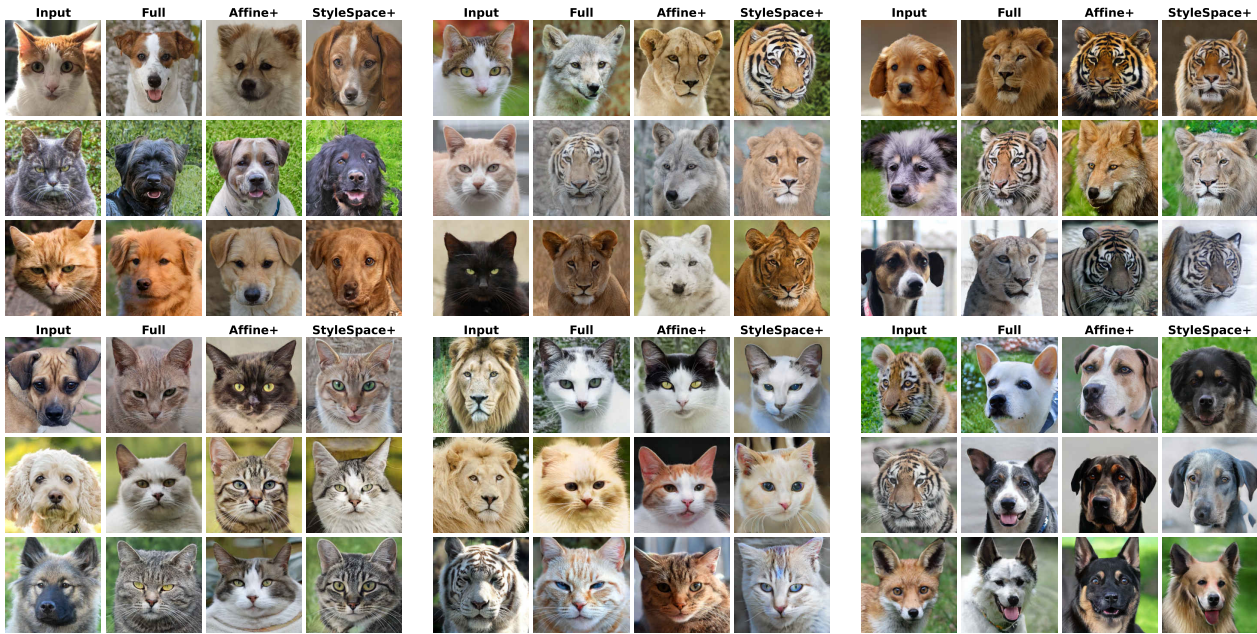
### A.6. Cross-domain image translation

We provide additional results for the image-to-image translation task for other datasets pairs complimentary to Figure 9 and describe the exact experimental setup.

We use the following approach to solve the I2I task (the same as in [42]): first, we invert a source image to the  $Z_{opt}$  latent space using a source domain generator. Then, we feed this representation to a generator in the target domain. In a reference-based setup, we additionally use the target generator to obtain the latent code for a reference image and then combine the first 6 style codes from the source image with the latest codes from the reference image. We perform 1000 optimization steps with truncation  $\psi = 0.7$ , and we use truncation  $\psi = 0.8$  at inference time.

We use validation splits of the AFHQ datasets (500 images) for the source and reference images. For reference-based I2I, we randomly select 10 reference images for each source image.

Figure 36 confirms that StyleSpace+ and Affine+ can transfer pose and style from the source image to the image in the target domain. Interestingly, Affine+ seems to preserve style a bit worse than the Full or StyleSpace+ parameterizations (most notably for the Cat target domain). For reference-based I2I, Figure 37 shows that all parameterizations are comparable both quantitatively and qualitatively.



	Size	cat2dog		cat2wild		dog2cat		dog2wild		wild2cat		wild2dog	
		FID	KID×10 <sup>3</sup>	FID	KID×10 <sup>3</sup>	FID	KID×10 <sup>3</sup>	FID	KID×10 <sup>3</sup>	FID	KID×10 <sup>3</sup>	FID	KID×10 <sup>3</sup>
Full	60.6M	40.5	11.6	12.8	2.44	18.6	2.78	17.5	4.64	18.6	3.28	42.6	12.7
Affine+	10.2M	42.3	12.9	16.3	4.92	18.4	2.37	13.2	3.14	21.5	3.18	41.4	10.6
StyleSpace+	1.1M	54.8	24.9	25.4	11.2	21.5	5.00	19.9	6.09	21.5	3.49	53.8	22.0

Figure 36. Comparison of I2I translation for different parameterizations. I2I with the generator in  $S+$  demonstrates the ability to capture the pose and the style from the source image while producing natural-looking results despite the presence of a gap in the metrics. At the same time, Affine+ parameterization can significantly reduce this gap.





	Size	cat2dog		cat2wild		dog2cat		dog2wild		wild2cat		wild2dog	
		FID	KID $\times 10^3$	FID	KID $\times 10^3$	FID	KID $\times 10^3$	FID	KID $\times 10^3$	FID	KID $\times 10^3$	FID	KID $\times 10^3$
Full	60.6M	25.1	12.5	9.03	2.59	7.64	2.22	11.9	3.60	7.71	2.52	24.0	11.5
Affine+	10.2M	21.8	7.33	5.79	0.80	8.44	2.53	5.59	0.78	8.44	2.32	20.9	7.00
StyleSpace+	1.1M	28.3	13.6	7.92	1.65	10.6	3.43	8.13	1.71	10.2	3.32	28.6	14.1

Figure 37. Comparison of reference-based image translation for different parameterizations. All three variants produce realistic images that combine pose and structure from the source image with texture and color from the reference. A quantitative comparison in the table above indicates parity between different parameterizations.

## A.7. Cross-domain image morphing

We provide more examples of complex cross-domain image morphing in Figures 38 to 41. Each complex image morphing is represented by 4 rows. First row represents cross-domain image morphing via smoothly adding StyleDomain direction in FFHQ domain. Second row shows cross-domain image morphing via weights interpolation between aligned generators with fixed StyleDomain direction. The third row demonstrates gradual interpolation between two StyleDomain directions that correspond to two different domains. Fourth row represents backward StyleGAN2 weight interpolation to FFHQ domain with fixed StyleDomain direction. There are two examples of cross-domain image morphing in each Figure.

We observe that transitions are very smooth and by leveraging properties of StyleDomain directions we can obtain complex cross-domain image morphing.

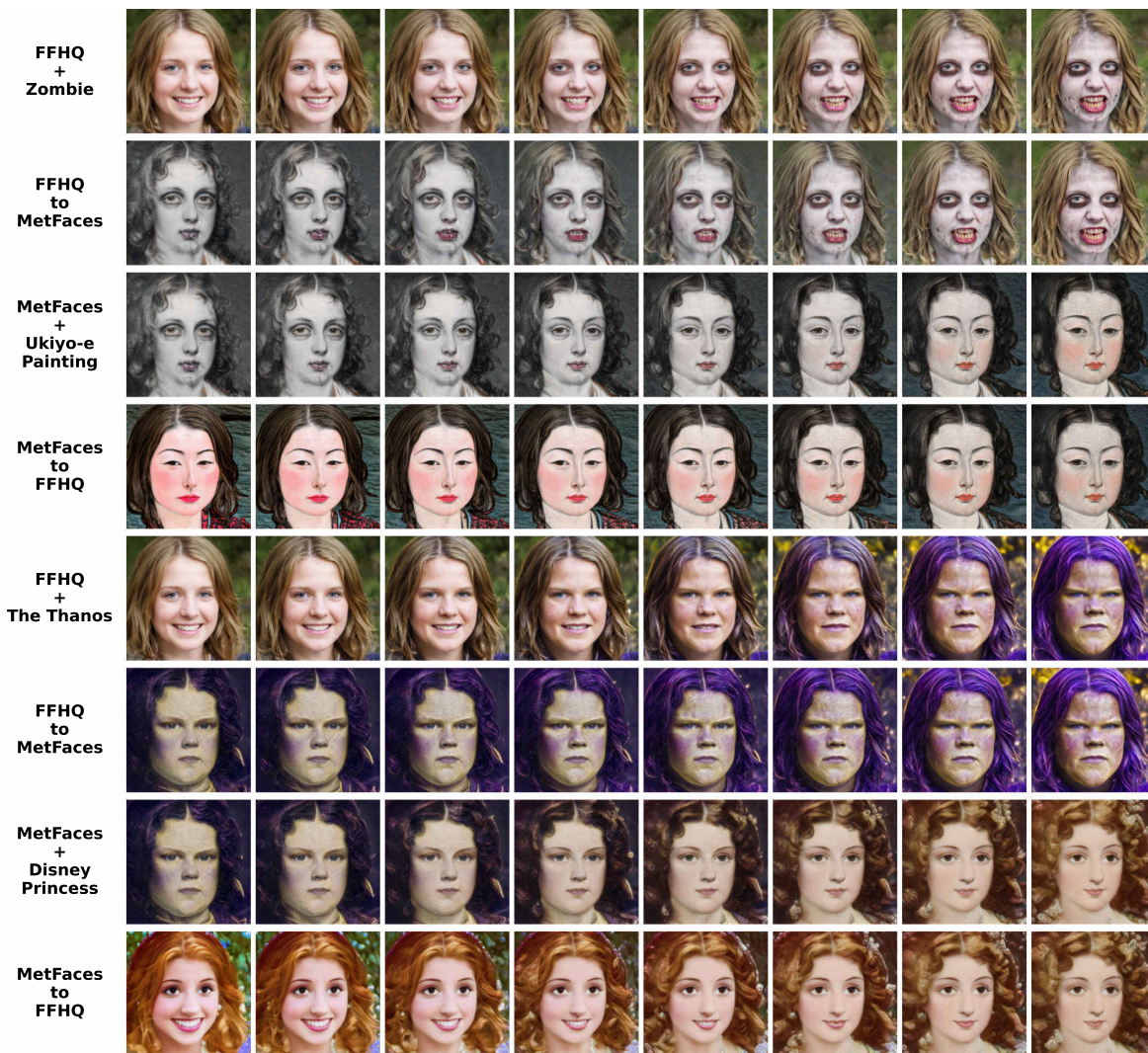


Figure 38. Example of complex cross-domain image morphing.

The first four lines represent "FFHQ  $\rightarrow$  FFHQ + *Zombie*  $\rightarrow$  MetFaces + *Zombie*  $\rightarrow$  MetFaces + *Ukiyo-e Painting*  $\rightarrow$  FFHQ + *Ukiyo-e Painting*".

The second four lines represent "FFHQ  $\rightarrow$  FFHQ + *The Thanos*  $\rightarrow$  MetFaces + *The Thanos*  $\rightarrow$  MetFaces + *Disney Princess*  $\rightarrow$  FFHQ + *Disney Princess*".



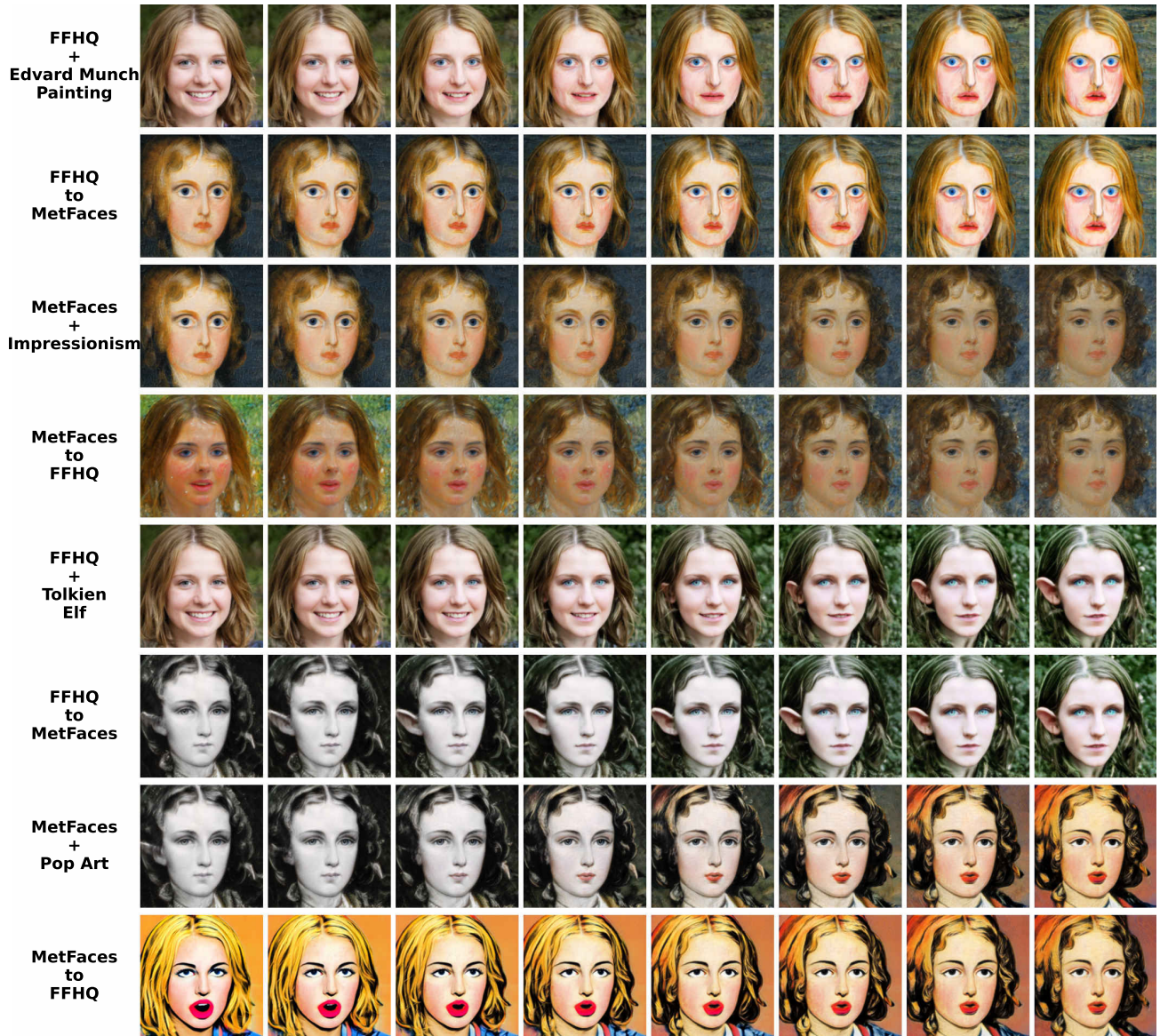


Figure 39. Example of complex cross-domain image morphing.

The first four lines represent " $FFHQ \rightarrow FFHQ + \text{Edvard Munch Painting} \rightarrow \text{MetFaces} + \text{Edvard Munch Painting} \rightarrow \text{MetFaces} + \text{Impressionism} \rightarrow FFHQ + \text{Impressionism}$ ".

The second four lines represent " $FFHQ \rightarrow FFHQ + \text{Tolkien Elf} \rightarrow \text{MetFaces} + \text{Tolkien Elf} \rightarrow \text{MetFaces} + \text{Pop Art} \rightarrow FFHQ + \text{Pop Art}$ ".



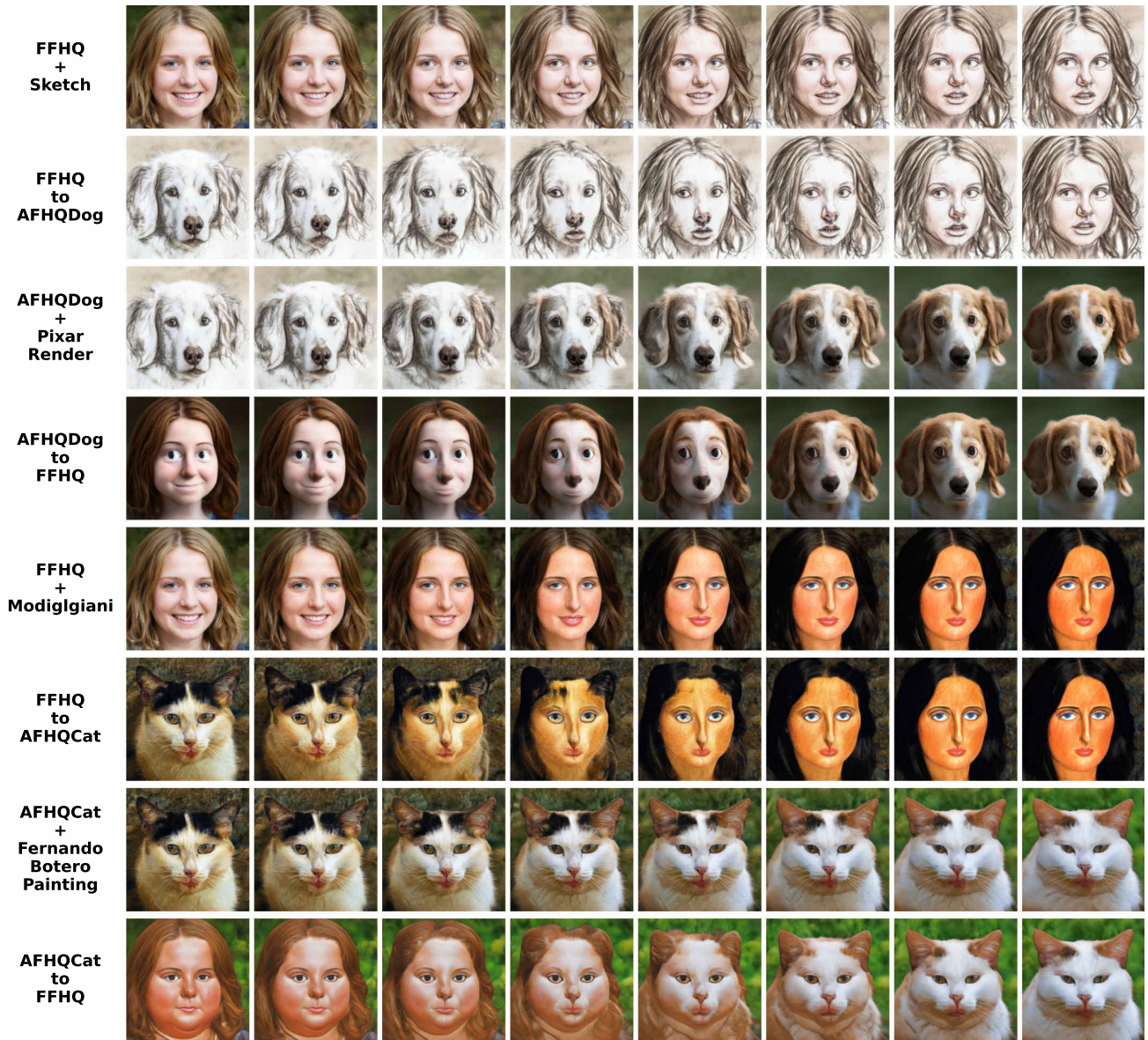


Figure 40. Example of complex cross-domain image morphing.

The first four lines represent " $FFHQ \rightarrow FFHQ + Sketch \rightarrow AFHQDog + Sketch \rightarrow AFHQDog + Pixar Rendering \rightarrow FFHQ + Pixar Rendering$ ".

The second four lines represent " $FFHQ \rightarrow FFHQ + Modigliani \rightarrow AFHQCat + Modigliani \rightarrow AFHQCat + Fernando Botero Painting \rightarrow FFHQ + Fernando Botero Painting$ ".



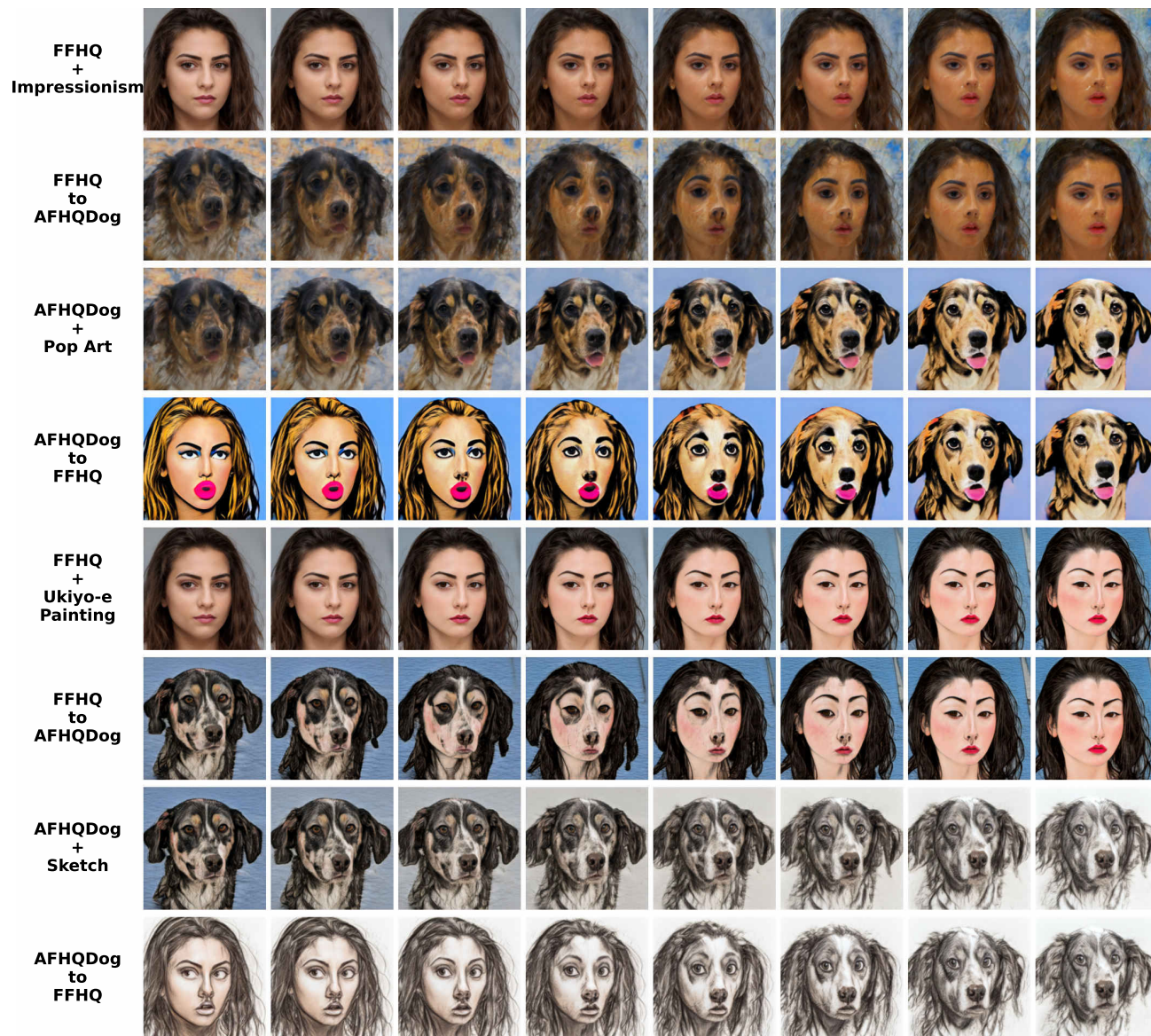


Figure 41. Example of complex cross-domain image morphing.

The first four lines represent "FFHQ  $\rightarrow$  FFHQ + Impressionism  $\rightarrow$  AFHQDog + Impressionism  $\rightarrow$  AFHQDog + Pop Art  $\rightarrow$  FFHQ + Pop Art".

The second four lines represent "FFHQ  $\rightarrow$  FFHQ + Ukiyo-e Painting  $\rightarrow$  AFHQDog + Ukiyo-e Painting  $\rightarrow$  AFHQDog + Sketch  $\rightarrow$  FFHQ + Sketch".